Atmos. Chem. Phys. Discuss., 14, 6663–6720, 2014
www.atmos-chem-phys-discuss.net/14/6663/2014/
doi:10.5194/acpd-14-6663-2014

Atmospheric Chemistry and Physics Discussions

Impacts of climate and emission changes on nitrogen deposition in Europe: a multi-model study

D. Simpson[1,2], C. Andersson[3], J. H. Christensen[4], M. Engardt[3], C. Geels[4], A. Nyiri[1], M. Posch[5], J. Soares[6], M. Sofiev[6], P. Wind[1,7], and J. Langner[3]

[1]EMEP MSC-W, Norwegian Meteorological Institute, Oslo, Norway
[2]Dept. Earth & Space Sciences, Chalmers University of Technology, Gothenburg, Sweden
[3]Swedish Meteorological and Hydrological Institute, Norrköping, Sweden
[4]Department of Environmental Science, Aarhus University, 4000 Roskilde, Denmark
[5]National Institute for Public Health and the Environment (RIVM), Bilthoven, the Netherlands
[6]Finnish Meteorological Institute, P.O. Box 503, 00101 Helsinki, Finland
[7]University of Tromsø, 9037 Tromsø, Norway

Received: 28 January 2014 – Accepted: 11 February 2014 – Published: 13 March 2014

Correspondence to: D. Simpson (david.simpson@met.no)

Published by Copernicus Publications on behalf of the European Geosciences Union.

Abstract

The impact of climate and emissions changes on the deposition of reactive nitrogen (Nr) over Europe was studied using four offline regional chemistry transport models (CTMs) driven by the same global projection of future climate over the period 2000–2050. Anthropogenic emissions for the years 2005 and 2050 were used for simulations of both present and future periods in order to isolate the impact of climate change, hemispheric boundary conditions and emissions, and to assess the robustness of the result across the different models.

The results from these four CTMs clearly show that the main driver of future N-deposition changes is the specified emission change. Under the specified emission scenario for 2050, emissions of oxidised nitrogen were reduced substantially, whereas emissions of NH_3 increase to some extent, and these changes are largely reflected in the modelled concentrations and depositions. The lack of sulphur and oxidised nitrogen in the future atmosphere results in a much larger fraction of NH_x being present in the form of gaseous ammonia.

Predictions for wet and total deposition were broadly consistent, although the three fine-scale models resolve European emission areas and changes better than the hemispheric-scale model. The biggest difference in the models is for predictions of individual N-compounds. One model (EMEP) was used to explore changes in critical loads, also in conjunction with speculative climate-induced increases in NH_3 emissions. These calculations suggest that the area of ecosystems which exceed critical loads is reduced from 64 % for year 2005 emissions levels to 50 % for currently estimated 2050 levels. A possible climate-induced increase in NH_3 emissions could worsen the situation, with areas exceeded increasing again to 57 % (for a 30 % NH_3 emission increase).

ACPD
14, 6663–6720, 2014

1 Introduction

As noted in Langner et al. (2012b), air pollution is still a major problem in Europe, with levels of gases and particles frequently exceeding target values. Many sensitive ecosystems are adversly affected by deposition of reactive nitrogen (Nr) from the atmosphere to vegetation and water bodies (Erisman et al., 2013; Sutton et al., 2011). Nr comprises both oxidised and reduced compounds, generally indicated by NO_y and NH_x respectively. Important NO_y compounds are NO and NO_2 (together known as NO_x) as well as species such as HNO_3 or particulate nitrates. The dominant NH_x compounds are gaseous ammonia (NH_3) and particulate ammonium, the latter usually associated with either sulphates or nitrate. Although emissions of NO_x in Europe are expected to keep decreasing in future, emissions of NH_3 may well increase in line with agricultural activities. An important new realisation is that increased temperatures associated with climate change may induce additional NH_3 emissions through increased evaporation (Skjøth and Geels, 2013; Sutton et al., 2013); these studies suggest possible increases of 20–50 % over the next century.

Changes in atmospheric circulation due to climate change can also affect future levels of air pollution and Nr deposition (e.g. Engardt and Langner, 2013, and references cited therein). Changes in meteorological conditions further influence local dispersion and deposition conditions to vegetation and thereby influence the effects of both long-range transported and locally emitted air pollutants on human health and ecosystems. Since the 1990s the concentration of S-components in the Arctic has declined, while the pattern for N-components is more complex showing both positive and negative trends. These interannual variations reflects the significant reductions in sulphur emissions in North America and Europe as well as interannual variations in synoptic transport and precipitation (Hole et al., 2009).

The link between climate change and air pollution in Europe has been assessed in several recent studies using regional CTMs (e.g. Langner et al., 2005, 2012a, b; Forkel and Knoche, 2007; Hedegaard et al., 2008; Andersson and Engardt, 2010;

ACPD
14, 6663–6720, 2014

Colette et al., 2012; Engardt and Langner, 2013). The majority of these studies have focussed on ozone concentrations, but for example Hole and Engardt (2008), Langner et al. (2009), Hedegaard et al. (2013) and Engardt and Langner (2013) presented some results for nitrogen species. Likewise, a number of studies have made projections of the future N deposition in Europe and the Arctic which included emission changes (e.g. Hole et al., 2009; Geels et al., 2012b; Engardt and Langner, 2013; Tuovinen et al., 2013, the latter using EMEP model results from the present exercise).

Several multi-model studies of atmospheric chemistry and long-range transport of air pollution in Europe have been carried out over the last decade (e.g. Vautard et al., 2006, 2007; van Loon et al., 2007; Cuvelier et al., 2007; Thunis et al., 2007; Colette et al., 2011; Solazzo et al., 2012; Dore et al., 2013), also at the hemispheric scale (Dentener et al., 2006; Sanderson et al., 2008). These studies have focused on establishing the robustness of model predictions in the present climate, although Lamarque et al. (2005) used global scale models with projections up to 2100.

Here we assess the combined uncertainty of predicting future climate, emissions and atmospheric chemistry and long-range transport of Nr over Europe, using finer-scale climate projections than used in previous studies, and with common emissions and meteorological systems. This study complements that of Engardt and Langner (2013), which used one CTM (MATCH) and examined the effects of using different meteorological drivers. Here we take a multi-model approach using four state-of-the-art offline CTMs to assess the uncertainty/robustness of model predictions of nitrogen deposition over Europe. Specifically, we evaluate the sensitivity of simulated Nr-deposition over Europe to changes in climate, changes in boundary conditions, and to emissions.

This study is a follow-up to the ozone study of Langner et al. (2012b), and largely follows the same methodology except in three respects: (i) the emission inventories were updated (see Sect. 2.1), making use of recent improvements in data-sets and finer-scale spatial distributions to provide more accurate model inputs, (ii) we have investigated the effects of emissions changes as well as of climate change, and (iii) considered 20 yr time-windows of simulation instead of 10 yr. The choice of 20 yr

ACPD
14, 6663–6720, 2014

time-windows is primarily driven by the strong interannual variability in precipitation and resulting interannual variability in wet deposition in the CTMs. Using shorter simulation periods leads to deposition changes driven by climate change that are not significant for large areas of the simulation domain. The use of 20 yr time-windows also smooths some of the decadal variability present in the climate model output. An even longer time-window could have been considered but 20 yr was found to be a good compromise between computational effort and level of significance.

2 Methods

This study uses the same basic model chain as in the ozone study of Langner et al. (2012b). Briefly, we focus on the comparison of Nr simulations from three European-scale CTMs, EMEP MSC-W, MATCH and SILAM, and one hemispheric CTM, DEHM. In order to obtain climate-sensitive meteorology, meteorological data from a global climate model (GCM) were used in both a regional climate model (RCM) and an offline hemispheric chemical transport model (DEHM). The downscaled meteorology from the RCM is used together with time-varying boundary conditions from the hemispheric DEHM CTM to drive the three European-scale CTMs. The horizontal grid for these CTMs was identical to the RCA3 grid, while the vertical discretization was left free to each model.

Three scenarios with the hemispheric model, and four scenarios with the European RCA3-driven CTMs, were needed to isolate and explore the effects of changing emissions, climate and boundary conditions, as summarised in Table 1. Emissions were either from the year 2005 or 2050 (which we denote "E05" and "E50"). Climate was investigated with differences in meteorology between that for 1990–2009 (which we denote the "2000s", or "M00") and 2040–2059 (the "2050s", or "M50"). Three sets of runs (denoted BC1, BC2, BC3) with the hemispheric DEHM model provided boundary conditions to the other CTMs for either the 2000s or 2050s periods, with the difference

ACPD
14, 6663–6720, 2014

between BC2 and BC3 reflecting changes in hemispheric emissions, particularly those of North America.

Two final scenarios are included in Table 1, E50X20-M50-BC3 and E50X30-M50-BC3, both of which are run with just one or two models as a more speculative exercise. These scenarios are added in order to address the possible increased emissions of ammonia resulting from increased temperatures (Skjøth and Geels, 2013; Sutton et al., 2013). This exercise will be discussed in Sects. 2.1.1 and 4. Details of the emission data, scenarios and models follow.

2.1 Emissions

The models used in this study require emissions of sulphur and nitrogen oxides (SO_x, NO_x), NH_3, non-methane volatile organic compounds (NMVOC), CO, and for DEHM CH_4. The anthropogenic emissions consist of annual, gridded, data-sets. Ten major types of anthropogenic emissions are used, classified with the so-called "SNAP"-level emission sectors (SNAP is Source Nomenclature of Air Pollutants, for example, SNAP-7 is road-traffic, SNAP-10 is agriculture, etc.).

In this study, all models made use of the same emission files, which contained gridded SNAP-level data on the RCA3 grid (and a global grid for DEHM). A number of emission inventories that became available in 2012 were merged for this study, aiming to provide consistency with data-bases used within the EU ECLAIRE project (http://www.eclaire-fp7.eu/) and best-possible spatial resolution for the underlying data. The latter aspect is important as the emissions need to be interpolated to the rotated latitude–longitude grid system of the RCA model, and the finer the base-grid the more accurate such interpolation can be.

A three-step procedure was used to generate the common emissions data-base used by all models. Firstly, national, SNAP-level, emissions were taken from the database produced by the International Institute for Applied System Analysis (IIASA) for various EU Projects and the Task Force on Hemispheric Transport of Air Pollution (Amann et al., 2013). The original (version 4) databases produced in 2011 were

ACPD
14, 6663–6720, 2014

updated in February 2012 for the ECLAIRE project. Secondly, for countries within the so-called MACC area (this includes all of the EU, plus some neighbours), the 7 km resolution MACC-2 emissions produced by TNO (Kuenen et al., 2011) were used to spatially distribute the country-specific SNAP emissions. For other countries the IIASA $0.5^{\circ} \times 0.5^{\circ}$ spatial resolution was preserved. Finally, international shipping emissions were added from the RCP6.0 data-sets (Hijioka et al., 2008).

Emission data-sets using this procedure were provided for the years 2005 and a 2050 "current legislation" (CLE) scenario. The EU totals are presented in Table 2. Figure 1 illustrates the 2005 emissions for NO_x and NH_3 in the RCA3 domain used by the three European-scale CTMs, and Fig. 2 shows the changes in emissions between 2005 and 2050. The changes for NO_x are dramatic across almost the whole EU area. In Germany for example, emissions decrease by nearly 70 %. Dramatic emissions increases are also seen in some areas, especially in North Africa and Turkey. For NH_3, the emission changes are more complex, with increases and decreases even within the EU area, and dramatic increases in especially some Russian areas.

A number of other emissions sources are typically used in the CTMs. These include so-called natural NO_x emissions from soils, NMVOC from vegetation, and emissions from forest-fires, aircraft and lightning. The CTMs have different approaches to these emissions sources, and harmonising these was beyond the scope of our study. Instead, in order to simplify the interpretation of the CTM results, we have adopted the simple policy of setting emissions from soils, forest-fires, aircraft and lightning to zero, so that all NO_x emissions in the models stem from the common emission data-set discussed above. In contrast to these minor emission sources, emissions of NMVOC from vegetation are too great to ignore (e.g. Simpson et al., 1999), and as in Langner et al. (2012b) each model simply calculates its own emissions at each model time-step. Similarly, volcanic emissions are a significant fraction of European S-emissions. The official EMEP estimate of volcanic emissions was used for all models.

ACPD
14, 6663–6720, 2014

2.1.1 A possible future – increased NH_3 emissions?

Two recent papers have drawn attention to the possibility of quite significant increases in NH_3 emissions in future, as a result of increasing evaporation from sources such as animal manure. These emissions are a function of both water availability and temperature with in principle a doubling of the emission for each 5 °C increase. Sutton et al. (2013), using empirical models and measurements estimated a potential 42 % increase in the global NH_3 emissions following a 5 °C increase towards 2100. Skjøth and Geels (2013) used a dynamic NH_3 emission model (Skjøth et al., 2011) to study the temporal and geographical variations in ammonia emissions across the Northern part of Europe. By using bias corrected ensemble mean surface temperatures from the ENSEMBLES project (van der Linden and Mitchell, 2009) the potential future changes in the emission from a typical Danish pig stable were tested in different locations and hence climates. Towards the 2050s a general increase of 15–30 % (relative to 2007) was found in the emissions in central to Northern Europe, increasing to ca. 20–40 % by the end of the century. It is reasonable to postulate that such increased emissions have the potential to offset many of the beneficial effects of European NO_y emissions reductions. The fact that more NH_x will be in the form of NH_3 rather than NH_4^+ (see Sect. 3.4) also suggests the possibility of quite large increases in near-source deposition if such emissions increases occur. The projected increase will of course depend heavily on the projected temperature change and hence on the applied climate model, as well as assumptions concerning NH_3 emission factors. However, based on the above studies we have chosen to explore the potential impact of a 20 % and 30 % increase in NH_3 emissions in our future period 2040–2059, in two scenarios denoted E50X20-M50-BC3 and E50X30-M50-BC3 (Table 1). Given the speculative nature of this exercise, we have used just the DEHM (for 20 %) and EMEP (for 20 and 30 %) models; with a focus on the impact of these scenarios on the critical loads calculations we will present in Sect. 4.

ACPD
14, 6663–6720, 2014

2.2 Climate-meteorology

Results of the global-scale ECHAM5 general circulation model (GCM) (Roeckner et al., 2006), driven by emissions from the SRES A1B scenario (Nakićenović, 2000), were downscaled over Europe with the Rossby Centre Regional Climate model (RCM), version 3 (RCA3) (Samuelsson et al., 2011; Kjellstrom et al., 2011). Details and discussion of both current and future climate simulated with RCA3 is given in Samuelsson et al. (2011) and Kjellstrom et al. (2011). Here we used the so-called ECHAM5-r3 downscaling from the SRES A1B emission scenario (see Kjellstrom et al., 2011, for details). The ECHAM5 version used is defined in spectral grid with truncation T63, which at mid-latitudes corresponds to a horizontal resolution of ca. 140 km (ca. 140 km × 210 km). The temporal resolution of the climate data was 6 hourly.

As in Langner et al. (2012b), the the horizontal resolution of RCA3 was 0.44° × 0.44° (ca. 50 km × 50 km) on a rotated latitude longitude grid, and data were provided with 6 hourly resolution. The climate as downscaled by RCA3 reflects broad features of the climate simulated by the parent GCM. The average temperature change in the period 2000–2040 predicted by RCA3 for the European model domain in the downscaled ECHAM5-r3 is 1.27 °C. This climate projection has a temperature change until the period 2040–2070 close to the average of an ensemble of 16 different projections downscaled from different GCM runs by RCA3 over Europe (Kjellstrom et al., 2011).

Figures S1 and S2 (see Supplement) illustrate the changes in temperature and precipitation between our 20 yr time-slices, from both the ECHAM-5 and RCA3 data. Although the general patterns of temperature are similar, the RCA3 temperature has clearly a higher spatial resolution than the ECHAM5 data, which is particularly obvious over the Alpine area. Temperature increases to the 2050s are somewhat greater in the ECHAM5 system.

For precipitation the increased resolution of RCA3 is also very evident. ECHAM5 has substantially more rainfall over most of Europe, but less so in some areas, e.g.

ACPD
14, 6663–6720, 2014

western Norway or the Alps. Both models show rather similar large-scale changes in precipitation to the 2050s though.

2.3 Chemical boundary conditions

As in Langner et al. (2012b), chemical boundary conditions at lateral and top boundaries of the regional models were provided by the hemsipheric DEHM model, which was also driven by the global ECHAM5-r3 meteorology. The boundary values taken from DEHM were updated every 6 h and interpolated from the DEHM resolution to the respective geometry of each regional CTM. To ensure consistency, the offline DEHM model was operated with global emissions for 2005 and 2050 from the same system as used for the European-scale CTMs.

2.4 The chemical transport models

The models used in this study have been introduced in our preceding multi-model study, Langner et al. (2012b). Here we just briefly review the models with focus on their handling of Nr compounds.

2.4.1 DEHM

The Danish Eulerian Hemispheric Model (DEHM) is a three-dimensional, Eulerian, CTM (Christensen, 1997; Frohn et al., 2002; Brandt et al., 2012; Geels et al., 2012a) developed at the Danish National Environmental Research Institute (now Aarhus University). The model domain covers most of the Northern Hemisphere, discretized on a polar stereographic projection, and includes a two-way nesting procedure with several nests with higher resolution over Europe, Northern Europe and Denmark (Frohn et al., 2002). In the vertical the model has 20 unevenly distributed layers defined in a terrain following sigma-level coordinate system with top at 100 hPa.

The chemical scheme comprises 58 photo-chemical compounds, 9 classes of particulate matter, and 122 chemical reactions. The original scheme by

ACPD
14, 6663–6720, 2014

(Strand and Hov, 1994) has been extended to include species relevant for the ammonium group chemistry. This includes ammonia (NH_3), ammonium nitrate (NH_4NO_3), ammonium bisulphate (NH_4HSO_4), ammonium sulphate ($(NH_4)_2SO_4$) and inorganic nitrates. Gaseous and aerosol dry deposition velocities are calculated based on the resistance method and is parameterized similar to the EMEP model (Simpson et al., 2003a; Emberson et al., 2000a) except for the dry deposition of species on water surfaces where the deposition depends on the solubility of the chemical species and the wind speed (Asman et al., 1994; Hertel et al., 1995). Wet deposition includes in-cloud and below-cloud scavenging and is calculated as the product of scavenging coefficients and the concentration in air.

Natural emissions of isoprene are calculated dynamically in the model according to the IGAC-GEIA biogenic emission model (International Global Atmospheric Chemistry – Global Emission Inventory Activity) (Guenther et al., 1995).

Background CH_4 concentrations were assumed to be 1760 ppb in all scenarios. As well as simplifying the interpretation of changes, this is consistent with John et al. (2012) who suggest that the atmospheric CH_4 is not projected to change much under all but the most extreme RCP scenarios. DEHM is regularly validated against observations of e.g. acidifying and eutrophying compounds (Brandt et al., 2012; Geels et al., 2012b, 2005).

2.4.2 EMEP MSC-W

The gaseous nitrogen species in the EMEP model which are subject to dry deposition are NO_2, HNO_2, HNO_3, PAN, MPAN and NH_3 (see Simpson et al., 2012, for explanation of PAN species). The surface resistance scheme is quite complex, featuring vegetation-specific corrections for phenology (time-of-year), temperature, humidity and soil water. The stomatal-uptake part of the scheme has been developed and tested for ozone in a series of papers (Emberson et al., 2001, 2000a, b, 2007; Klingberg et al., 2008; Simpson et al., 2001, 2003b; Tuovinen et al., 2001, 2004).

ACPD
14, 6663–6720, 2014

The bulk surface conductance in the EMEP model is calculated specifically for O_3, SO_2, and NH_3. Values for other gases (except HNO_3) are obtained by interpolation of the O_3 and SO_2 values. For ammonia and sulphur dioxide, deposition rates also depend on humidity levels, temperature, and an acidity ratio (defined as the molar ratio of $[SO_2]/[NH_3]$). These acidity ratios are a first attempt to account for the observed changes in resistance in areas with different pollution climates (Erisman et al., 2001; Fowler and Erisman, 2003; Fowler et al., 2009). For NO_2 the deposition velocity is reduced as air concentrations approach 4 ppb (a psuedo-compensation point). Further, NH_3 deposition is switched off over growing crops, a simple way to account for the bi-directional fluxes expected over such areas. For further details, see Simpson et al. (2012).

The particulate nitrogen species in the EMEP model which are subject to dry deposition are fine and coarse nitrate, and ammonium. Aerosol deposition in the EMEP model was considerably simplified in recent years. The new formulation (Simpson et al., 2012) uses a simple u_* dependence as in many studies (Wesely et al., 1985; Lamaud et al., 1994; Gallagher et al., 1997; Nemitz et al., 2004), but modified by an enhancement factor for nitrogen compounds in unstable conditions, see Simpson et al. (2012) for details. The settling velocities of coarse particles are calculated as in Binkowski and Shankar (1995). Comparison of EMEP model results with observations of acidifying compounds can be found in annual EMEP reports (www.emep.int), in several papers (Aas et al., 2012; Fagerli and Aas, 2008; Simpson et al., 2006a, b), and as part of a multi-model comparison in the UK (Dore et al., 2013).

2.4.3 MATCH

In this study, oxidised nitrogen in MATCH consists of the gases NO, NO_2, HNO_3, peroxyacetyl nitrate (PAN) and N_2O_5, particulate nitrate, NO_3-radicals and the isoprene-NO_3 adduct. Reduced nitrogen is NH_3 and particulate ammonium.

Wet deposition is, for most species, calculated as a height-varying scavenging coefficient times surface precipitation intensity. For ozone, hydrogen peroxide, and sulphur

ACPD
14, 6663–6720, 2014

dioxide, in-cloud scavenging is calculated by assuming Henry's law equilibrium; sub-cloud scavenging is neglected for these species. To calculate dry deposition, MATCH use a resistance approach, based on surface-type and atmospheric stability. Species that enter the stomata of plants (i.e. most gases) display a diurnal variation in surface resistance based on a specified, monthly varying, surface-type specific, non-stomatal deposition velocity plus a diurnally varying term that is zero during night and reach its specified maximum during local noon. In this study, we discriminate between four different surface-types: water, low vegetation, high vegetation (i.e. forest), barren land (including urban areas). For non-water surfaces the dry deposition velocity is decreased by low temperatures or snow cover. For ozone, the surface resistance is affected by photosynthetic active radiation, soil moisture and temperature (see Andersson and Engardt, 2010). Particulate matter and some gases have monthly varying dry deposition velocities that only vary according to land-surface. Numerical values of most dry deposition velocities and scavenging coefficients are given in Andersson et al. (2007).

Details of the numerics, boundary layer parameterization and deposition parameterization are given in (Robertson et al., 1999; Engardt, 2000). The chemistry, based upon Simpson et al. (1993), has strong links between Nr compounds and sulphur compounds, as well as ozone. The implementation is described in Langner et al. (1998), although several of the rate constants have been updated. The ability of MATCH to reproduce the concentration and deposition of acidifying and eutrophying species when forced by data from RCA3 is discussed in e.g. Engardt and Langner (2013) and Langner et al. (2009). In Andersson et al. (2007) MATCH is evaluated when forced with meteorology from ERA40.

2.4.4 SILAM

The SILAM model (System for Integrated modeLling of Atmospheric coMposition) is documented in Sofiev et al. (2008), Huijnen et al. (2010), Kukkonen et al. (2012). The system includes a meteorological pre-processor for evaluation of basic features of the boundary layer and the free troposphere using the meteorological fields provided by

ACPD
14, 6663–6720, 2014

Numerical Weather Prediction data (Sofiev et al., 2010). The physical-chemical modules of SILAM include several tropospheric chemistry schemes, description of primary anthropogenic and natural aerosols and radioactive processes. For the current study the transformation scheme utilised is the updated version of the DMAT chemical scheme (Sofiev, 2000), that incorporates the main formations pathways of secondary inorganic aerosols: the scheme covers 21 transported and 5 short-lived substances, which are interrelated via ca. 60 chemical reactions. Nitrogen components include NO, NO_2, N_2O_5, NO_3 radical, HONO, HNO_3, PAN, NH_3, NH_4NO_3 (in $PM_{2.5}$), $(NH_4)_{1.5}SO_4$ (in $PM_{2.5}$ and PM_{10}), and coarse nitrates formed on the surface of sea salt particles, Here $(NH4)_{1.5}SO_4$ denotes an equal-fraction mixture of ammonium mono- and bisulphate. Formation and breakup of ammonium nitrate follows the temperature-dependent equilibrium parameterization suggested by Finlayson-Pitts and Pitts (2000).

The removal processes are described via dry and wet deposition. Depending on particle size, mechanisms of dry deposition vary from primarily turbulent diffusion driven removal of fine aerosols to primarily gravitational settling of coarse particles (Kouznetsov and Sofiev, 2012). Wet deposition distinguishes between sub- and in-cloud scavenging by both rain and snow (Sofiev et al., 2006; Horn et al., 1987; Smith and Clark, 1989; Jylhä, 1991). Meteorological information and necessary geophysical and land cover maps are taken from the meteorological fields. The results shown in this study are based on a vertical profile represented by 9 non-regularly spaced levels reaching up to the tropopause, the lowest layer is 25 m thick.

3 Results

In this section we first compare the base-case model simulations against observations, in order to establish reasonable model performance of the CTMs as driven by their GCM/RCM climate data, and then compare model predictions across Europe for the base case and scenario runs. It should be noted that the CTMs have different methods of producing near-ground concentrations for comparison to measurements. DEHM and

ACPD
14, 6663–6720, 2014

SILAM use the concentration of each model's lowest layer, this being 60 m and 25 m respectively. For the EMEP and MATCH models, 3 m concentrations are estimated from the model's lowest layer (ca. 45 m grid-center for EMEP, 30 m for MATCH), assuming similarity theory and deposition-induced vertical gradients (Simpson et al., 2012; Robertson et al., 1999).

3.1 Comparison with observations

Observed concentrations of nitrogen and sulphur compounds in air and precipitation were extracted from the EMEP database (http://www.emep.int; Tørseth et al., 2012) for the years 2000–2010. Observed means were constructed for the period, with the criteria of 80 % capture per year over at least five years in 11 yr. For the four CTMs, modelled 20 yr means (1990–2009 climate; 2005 emissions) were constructed for the measurement sites reaching this criteria. The resulting paired data were evaluated for statistical performance using relative bias (%bias), Pearson correlation coefficient (R) and root mean square error (RMSE). The evaluation includes air concentrations of gaseous and aerosol sulphur and nitrogen species (Table 3), and deposition and concentration in precipitation of oxidised sulphur and oxidised and reduced nitrogen (Table 4). Evaluation of precipitation, from ECHAM5 (for DEHM) and from RCA3 (for the three European-scale CTMs), is also included in the evaluation (Table 4).

It is important to note that we cannot expect CTM models driven by GCM or RCM meteorology to perform as well as they would with data from Numerical Weather Prediction (NWP) models; the latter are the result of assimilating observed data into dedicated meteorological models. The ECMWF IFS model for example continuously assimilates near-surface, airborne and satellite observations to ensure good performance. This NWP model has a spatial resolution of about 16 km, and in standard usage the EMEP model updates IFS data every 3 h. In contrast, the RCA3 data has a spatial resolution of about 50 km, is updated every 6 h, and has no assimilation of observations. The comparison results presented in Tables 3–4 are thus not designed to reflect optimum model performance, but rather to show that despite the limitations of RCM meteorology,

ACPD
14, 6663–6720, 2014

the CTM models still do a reasonable job of reproducing concentration and deposition levels on a statistical basis.

From Table 3 it is clear that most models do a fair job of capturing SO_2 and NO_2 concentrations, but results are mixed for the other compounds. The underprediction of NH_3 is expected for all models as the lowest model layers (between 25–60 m thick) will not resolve vertical gradients caused by NH_3 emissions, and since measurements are often affected by nearby agricultural sources, but EMEP and MATCH show the largest negative bias. The largest discrepancies in the concentrations are seen for some aerosol (or sum of gas + aerosol) components, for example both SILAM and DEHM overestimate total nitrate by a factor of two. For wet deposition (Table 4), results are also mixed, but most results are within 30 %.

The results for DEHM in this setup were investigated in more detail since previous model evaluations, which usually use meteorological data from the MM5 model, show significantly better agreement with measured concentrations (Brandt et al., 2012; Geels et al., 2005). A thorough evaluation of DEHM driven by climate data from an earlier version of the ECHAM model (ECHAM4) also showed a reasonable agreement with EMEP observations (Hedegaard et al., 2008). The main reason for the poorer performance in this study seems to be very low values for the mixing height. In DEHM the mixing height is in the current setup described by a simple energy balance expression using information on e.g. the sensible heat flux and the friction velocity from the ECHAM5 model (Christensen, 1997). A comparison between DEHM and the EMEP model show that the mixing height in DEHM is only 20–60 % of the height in EMEP over the Mediterranean and most of the western part of Europe (see Fig. S3, Supplement). When using a setup with the MM5 model, we also get a significant higher mixing height in DEHM.

3.2 Deposition maps, base-case

Figure 3 presents the results of the four models for total Nr deposition. Patterns of Nr deposition are seen to be generally similar across the four models, with high

ACPD
14, 6663–6720, 2014

depositions over the major emission areas in Northern Italy and the Benelux area. The DEHM model shows smoother gradients, a result of being driven by the larger scale (and lower resolution) ECHAM meteorological driver. These results are also summarised in Table 5. This Table also includes the "3CTM-ensemble" mean and spread, with this small ensemble consisting of the three fine-scale models EMEP, MATCH and SILAM. (DEHM was excluded from the ensemble since its larger-scale and lower spatial resolution make its results somewhat different to the RCA3 driven CTMs.) Table 5 shows similar values for the total deposition of Nr from the different models, with a range between 6.7 to 9.0 kg (N) ha^{-1}. The contributions from NO_y and NH_x are almost equal as an ensemble mean, although the models differ somewhat in their ranking of these components. The largest differences between the 3CTM-ensemble models and DEHM are seen for the dry-deposition components, with factor of two differences. This is likely a result of the lower mixing heights in DEHM discussed in Sect. 3.1 (cf. Supplement, Fig. S3). SILAM shows the highest levels of NO_y deposition (especially wet) among the four CTMs, but the lowest deposition of NH_x.

Such differences are not unexpected, as chemical mechanisms, deposition process, and dispersion processes are quite different in the four CTMs. As a further illustration of this, Fig. 4 shows concentrations and dry-depositions of NO_2 and NH_3 along the north-south European transect at 10° E indicated in Fig. 1 (this transect was chosen as it passes through many different pollution climates, from the polluted Po valley in the south, through high NH_3 areas in NW Europe, to relatively clean areas in the north). Differences are clearly substantial, with for example EMEP showing far lower deposition rates of NO_2 compared to especially MATCH and SILAM, despite relatively high NO_2 concentrations. This particular feature likely reflects the EMEP model's use of lower deposition velocities as a proxy for an NO_2 compensation point (this behaviour is switched on when there is no explicit modelling of soil NO emissions). Such model assumptions can have large impacts on individual species, although a lower impact on total Nr concentrations or depositions.

ACPD
14, 6663–6720, 2014

3.3 Scenario runs

Figure 5a shows the 3CTM-ensemble mean NO_y deposition from the three RCA3-driven European-scale CTMs, with levels of around 5–10 kg(N) ha^{-1} in central Europe, declining to less than 2 kg(N) ha^{-1} in northern areas. Figure 5b shows the changes in NO_y deposition arising from climate change only (E05-M00-BC2). Levels of NO_y deposition increase in central Europe to some extent (ca. 0.1–0.5 kg(N) ha^{-1}), but decrease in for example the Nordic area by a similar amount. Figure 5c shows the corresponding changes brought about by scenario E05-M50-BC3, in which boundary conditions are also allowed to change to 2050 levels, but the picture is little changed from the effects of climate change alone. Figure 5d shows much more dramtic changes in the case of E50-M50-BC3, where European emissions are set to the 2050 levels. NO_y deposition is reduced by more than 0.5 kg(N) ha^{-1} over almost all of Europe, and more than 4 kg(N) ha^{-1} in central areas.

Figure 6 provides similar results for NH_x deposition. The results of the climate and climate+boundary-conditions simulations are rather similar in magnitude to the equivalent results for NO_y species, although climate change seems to increase NH_x in northern and eastern regions to a greater extent than NO_y. In broad terms, these climate-related runs seem to reflect the pattern of rainfall change (Fig. S2d, Supplement) to some extent. The most dramatic difference is though with Fig. 6d which shows that future emissions will substantially increase NH_x deposition in large parts of Europe (discussed further below).

Figure 7 summarises the results of these calculations, presenting average depositions over the inner-domain (cf. Fig. 1) from all four models, and four scenarios. As noted above in the spatial maps, the most dramatic changes are only seen with the E50-M50-BC3 scenario in which emissions from the year 2050 are used. Dry and wet deposition of NO_y decreases significantly in all models. Dry deposition of NH_x increases to some extent in all models, whereas wet deposition of NH_x shows smaller changes.

ACPD
14, 6663–6720, 2014

The similarity of results from the three scenarios using 2005 emissions from each model is unsurprising, given that emissions are not changed, and the domain is large, but differences are much more apparent when looking at smaller regions or particular locations. In order to visualise this better, Figs. 8 and 9 show the Nr-deposition and changes in Nr-deposition along the same north-south transect as used in Fig. 4). In Fig. 8, the densely populated (and high emission, especially for NH_3) Italian Po Valley area, starting around 45° N is clearly visible in the three RCA3-driven CTMs. The ECHAM5-driven DEHM model shows smoother deposition patterns, but all models show high Nr-deposition from around 45° N to around 58° N (between Denmark and Norway). Differences in Nr-deposition are greatest for the dry deposition components along this transect, with for example a factor of three between the lowest and highest values in mid-latitudes.

Figure 9 shows the differences between the future case (E50-M50-BC3) and base-case for the same components. The models are seen to behave in rather similar ways for total and wet-deposition, with substantial reductions (of up to 10 kg(N) ha^{-1}) in the Po valley region. For dry deposition, the picture is more complex, with larger differences between models, and with some regions experiencing reduced Nr-deposition, others (e.g. around 55° N) experiencing increased deposition.

3.4 Changes in NH_x partitioning

Results presented so far have dealt with groups of either oxidised, reduced, or total depositions of Nr compounds. Figure 10 illustrates changes for particular compounds, from one model (EMEP). The oxidised compounds, NO, NO_2, and nitrate all show relatively straightforward reductions, as expected from the emissions change. PAN is also reduced, but not to the same extent, and PAN also shows more sensitivity to the climate and boundary condition changes than other NO_y species. The most interesting changes are seen for the reduced compounds, however, with substantial increase in gaseous NH_3 and substantial decreases in particulate ammonium. This effect was also noted by Engardt and Langner (2013) and is caused by the fact that in the year 2050

ACPD
14, 6663–6720, 2014

scenarios, there is too little sulphate and even too little HNO_3 to react with NH_3. This effect if further illustrated in Fig. 11, which shows the changes in (a) NH_3 deposition and (b) total NH_x deposition between the base and future case. Comparing these changes to Fig. 2b, it is clear that while the total NH_x deposition change is quite similar to that of the emissions, the deposition of NH_3 is clearly much higher than the emission change in much of Europe. There are of course many issues with the modeling of ammonia exchange, with clear model limitations associated with the lack of bi-directional exchange in these CTMs (Bash et al., 2013; Flechard et al., 2013; Wichink-Kruit et al., 2010). This will be discussed further in the Conclusions. The results of the increased NH_3 emissions associated with the final two scenarios are discussed below in the context of critical load exceedances.

4 Exceedances of critical loads

A critical load (CL) is defined as a quantitative estimate of an exposure to one or more pollutants below which significant harmful effects on specified sensitive elements of the environment do not occur according to present knowledge (Nilsson and Grennfelt, 1988). If a deposition is higher than the critical load at a site, the CL is said to be exceeded; and in this paper, exceedances due to total annual N deposition are calculated for the region of the EU28 plus Norway and Switzerland (EU28+CH+NO, or $EU28^+$ for short). Dentener et al. (2006) and Lamarque et al. (2005) used a fixed, ecosystem independent, CL value of $1\,g(N)m^{-2}\,yr^{-1}$ ($10\,kg(N)\,ha^{-1}\,yr^{-1}$), as this allowed comparison across multiple models. Before we consider calculations of "real" ecosystem-dependent CL values with the EMEP model, we present first also our multi-model comparison using this simple $10\,kg(N)\,ha^{-1}$ value. Table 6 compares the area of exceedance of $10\,kg(N)\,ha^{-1}\,yr^{-1}$ (f_{10}) and the average exceedance (E_{10}) for all scenarios used in this study, including the X20 and X30 variations of the future case. Table 6 shows that the three European-scale CTMs give similar areas of exceedance of the $10\,kg(N)\,ha^{-1}\,yr^{-1}$ level (ca. 40 %) in the base-case, although MATCH

ACPD
14, 6663–6720, 2014

predicts considerably more excess than EMEP. DEHM shows a much larger area of exceedance, and excess, in this case. Similar to results presented above for total depositions, the effect of the E05-M50-BC2 and E05-M50-BC3 scenarios is relatively small. The E50-M50-BC3 scenario shows dramatic reductions in f_{10} and E_{10} compared to the base-case.

The DEHM and EMEP models were used for the future scenario with 20 % increased NH_3 emissions (E50X20-M50-BC3). Although exceedances are still below the base-case values, the increased NH_3 has a large impact, with 50 % and 80 % increases in E10 compared to the standard future scenario E50-M50-BC3. The EMEP model calculation of the 30 % NH_3 increase brings E_{10} values almost back to the 2005 levels.

As noted above, the use of the fixed 10 kg(N) ha^{-1} yr^{-1} threshold is a simple proxy for CLs. Within the Convention for the Long-range Transboundary Air Pollution (CLRTAP, www.unece.org/env/lrtap), for which EMEP provides ecosystem-specific deposition data, CL values are assessed in a much more realistic way. Critical loads are calculated for different receptors (e.g., terrestrial ecosystems, aquatic ecosystems); and "sensitive elements" can be any part (or the whole) of an ecosystem or ecosystem process. Critical loads have been defined for several pollutants (S, N, heavy metals), but here we restrict ourselves to CLs defined to avoid the eutrophying effects of N deposition (critical load of nutrient N, $CL_{nut}(N)$). The CL for a site is either derived empirically or calculated from a simple steady-state mass balance equation(s) that link a chemical criterion (e.g. an acceptable N concentration in soil solution that should not be exceeded) with the corresponding deposition value(s). Methods to compute CLs are summarised in the so-called Mapping Manual (UNECE, 2004; De Vries and Posch, 2003).

Values of $CL_{nut}(N)$ are calculated using the current critical load database held at the Coordination Centre for Effects (CCE; Posch et al., 2011, 2012) and used in supporting EU and CLRTAP negotiations on emission reductions (Hettelingh et al., 1995, 2001; Reis et al., 2012). The single exceedance number computed for a grid cell (or any other region) is the so-called average accumulated exceedance (AAE), defined as the

ACPD
14, 6663–6720, 2014

weighted mean of all ecosystems within the grid, with the weights being the respective ecosystem areas (see Posch et al., 2001).

Figure 12 shows the grid AAE values, as derived from the EMEP model ecosystem-specific N deposition data for the six scenarios (cf. Table 1). Although reductions in exceedance are seen in especially the E50-M50-BC3 scenario compared to the base-case, patterns do not vary dramatically, and even for this most stringent scenario there is still widespread exceedance. To summarise better these scenarios, the inverse cumulative distribution functions of the exceedances are shown in Fig. 13. Exceedances for the three scenarios distinguished only by meteorology and/or boundary condition are similar (see also Table 7 for some statistics), whereas the change in emissions has (obviously) the largest overall impact. Exceedance levels for the X20 and X30 versions of the 2050 scenarios are well below the scenarios representative of the 2000s, but substantially greater than the E50-M50-BC3 case.

5 Conclusions

This study has compared predictions of nitrogen deposition from four chemical transport models (CTMs), for both current conditions and future scenarios. All models were driven by the same basic emission system (except for biogenic VOC, which was model specific). The three European scale CTM models were driven by the same regional climate model (RCA3) meteorology, and also by a common set of boundary conditions given by the fourth (hemispheric-scale) CTM, DEHM. One base-case and three main scenario cases were designed to explore the impact of climate, boundary conditions, and emissions changes on European N-deposition. Two further speculative scenarios were also explored with 1–2 models.

As all of these models have been driven by data from global and/or regional climate models, rather than "real" NWP meteorology, it is not possible to directly compare to measurements. However, we have compared modelled and observed data in a statistical way, and in general the model results seem comparable to the observations (most

ACPD
14, 6663–6720, 2014

components were predicted within 30 %). Some significant discrepancies were found, which in the case of the DEHM model could be ascribed to problems caused by the large-scale climate data that are not normally seen in typical DEHM usage.

Deposition estimates from the models were compared as large-scale average, and illustrated for a north-south transect. Although modelled total deposition was rather similar among the models (presumably reflecting prescribed emissions), differences for wet or dry contributions were typically of the order of 30 %. For specific locations (as illustrated along our transect), or even more so for specific compounds, differences can be much greater. Of course, such differences are not unexpected since many aspects of Nr modelling are not well constrained. For example, there is a lack of data which could specify the proper partitioning of NO_y between HNO_3 and fine or coarse nitrate. Further, large variability in dry deposition rates (with factors of 2–3) is known to exist among deposition modules (Flechard et al., 2011). This variability is a reflection of the difficulties in measuring deposition rates (e.g. Fowler et al., 2009; Pryor et al., 2008) and also of complications due to bi-directional fluxes (discussed below) and chemical interactions. There is thus a lack of data with which to constrain dry-deposition rates, and this is reflected in the differences in modelled Nr depositions found in this study.

Other results from the model comparison can be summarised:

- All models clearly show that the impact of emissions changes is much greater than the impact of climate change alone, or of both climate change and emissions changes outside of Europe.
- The biggest difference between the models is for predictions of individual N-compounds. Predictions for wet and total deposition were, however, broadly consistent, although the three fine-scale models resolve European emission areas and spatial changes better than the hemispheric-scale model.
- The model predictions for 2050 generally follow the emission changes, with significant reductions in oxidised N concentrations and depositions, but slightly increasing levels of reduced N-deposition.

ACPD
14, 6663–6720, 2014

– For reduced nitrogen, the 2050 emissions are predicted to cause a large increase in gaseous NH_3 deposition in most of Europe, but with large corresponding decreases in ammonium. This difference is caused by the much reduced levels of both SO_2 and HNO_3 in the future atmosphere, preventing the formation of ammonium sulphates or nitrates.

– The ecosystem-specific depositions of the EMEP model were used to assess the extent to which critical loads (CLs) for ecosystems were exceeded in the different scenarios. The results showed that CLs were essentially only sensitive to scenarios which change emissions. In the 2050 future case, exceedances were substantially reduced, but were still widespread, with exceedances of CL in 50 % of ecosystems (mean exceedance of 1.89 kg(N) ha^{-1} yr^{-1}, down from 3.81 kg(N) ha^{-1} yr^{-1} in the base-case.).

– Two further scenarios were explored, involving 20 % and 30 % increases in NH_3 emissions above expected 2050 levels, which reflects the possibility that the emission rates might respond to climate change more than accounted for in the emissions inventory. Comparison of these runs against the CL data shows that even a 30 % increase in NH_3 will not bring exceedances back to 2000s levels, but such climate-induced increases cause CL exceedances which are substantially larger than those of the standard 2050 emission scenario (worst case here 57 % of areas in excess, with 2.9 kg(N) ha^{-1} yr^{-1} mean exceedance).

Major problems remain in predicting NH_3-deposition in particular. The complexities of bi-directional exchange have been noted in many papers (e.g. Sutton et al., 1995; Nemitz and Sutton, 2004; Fowler et al., 2009; Massad et al., 2010; Flechard et al., 2013), and some CTMs have attempted to include such exchange (e.g. Wichink-Kruit et al., 2010; Bash et al., 2013). As an example, Wichink-Kruit et al. (2012) showed that inclusion of bi-directional exchange increases the transport distance of NH_x, which would affect any predictions of Nr-deposition and CL-exceedance. However, such modelling is limited by many factors, including process-uncertainties (Massad et al., 2010; Flechard

ACPD
14, 6663–6720, 2014

et al., 2013), problems of sub-grid heterogeneity (e.g. Loubet et al., 2001, 2009), and lack of necessary and accurate input data.

Still, the overriding conclusion of this paper is probably robust: reducing future deposition of Nr in Europe is mainly dependent upon the way in which future NH_3 emissions develop. The new recognition that climate change may influence emissions much more than currently accounted for in official inventories makes it even more important that methods to deal with NH_3 emissions are improved.

Supplementary material related to this article is available online at http://www.atmos-chem-phys-discuss.net/14/6663/2014/acpd-14-6663-2014-supplement.pdf.

Acknowledgements. This study was initiated and mainly supported by the Nordic Council of Ministers (EnsCLIM project, NMR no. KoL-10-04) and EU project ECLAIRE (project no. 282910). Further support came from the EU projects MEGAPOLI (no. 212520), PEGASOS (no. 265148), TRANSPHORM (no. 243406), NMR FAN (kol-1204) and Danish ECOCLIM projects, and the Swedish Environmental Protection Agency through the research programme CLEO – Climate Change and Environmental Objectives as well as EMEP under the LRTAP UNECE Convention. The work is also a contribution to the Swedish Strategic Research Areas Modelling the Regional and Global Earth System (MERGE). Thanks are due to C. Heyes and Z. Klimont at IIASA for valuable help with the emission inventory processing.

References

Aas, W., Tsyro, S., Bieber, E., Bergström, R., Ceburnis, D., Ellermann, T., Fagerli, H., Frölich, M., Gehrig, R., Makkonen, U., Nemitz, E., Otjes, R., Perez, N., Perrino, C., Prévôt, A. S. H., Putaud, J.-P., Simpson, D., Spindler, G., Vana, M., and Yttri, K. E.: Lessons learnt from the first EMEP intensive measurement periods, Atmos. Chem. Phys., 12, 8073–8094, doi:10.5194/acp-12-8073-2012, 2012. 6674

ACPD
14, 6663–6720, 2014

Amann, M., Klimont, Z., and Wagner, F.: Regional and global emissions of air pollutants: recent trends and future scenarios, Annu. Rev. Env. Resour., 38, 31–55, doi:10.1146/annurev-environ-052912-173303, 2013. 6668

Andersson, C. and Engardt, M.: European ozone in a future climate: importance of changes in dry deposition and isoprene emissions, J. Geophys. Res., 115, D02303, doi:10.1029/2008JD011690, 2010. 6665, 6675

Andersson, C., Langner, J., and Bergstrom, R.: Interannual variation and trends in air pollution over Europe due to climate variability during 1958-2001 simulated with a regional CTM coupled to the ERA40 reanalysis, Tellus B, 59, 77–98, doi:10.1111/j.1600-0889.2006.00196.x, 2007. 6675

Asman, W. A. H., Sørensen, L. L., Berkowicz, R., Granby, K., Nielsen, H., Jensen, B., Runge, E., Lykkelund, C., Gryning, S. E., and Sempreviva, A. M.: Dry deposition processes, Danish Environmental Protection Agency, Marine Research, 35, Copenhagen, Denmark, 1994. 6673

Bash, J. O., Cooter, E. J., Dennis, R. L., Walker, J. T., and Pleim, J. E.: Evaluation of a regional air-quality model with bidirectional NH_3 exchange coupled to an agroecosystem model, Biogeosciences, 10, 1635–1645, doi:10.5194/bg-10-1635-2013, 2013. 6682, 6686

Binkowski, F. and Shankar, U.: The Regional Particulate Matter Model, 1. Model description and preliminary results, J. Geophys. Res., 100, 26191–26209, 1995. 6674

Brandt, J., Silver, J. D., Frohn, L. M., Geels, C., Gross, A., Hansen, A. B., Hansen, K. M., Hedegaard, G. B., Skjoth, C. A., Villadsen, H., Zare, A., and Christensen, J. H.: An integrated model study for Europe and North America using the Danish Eulerian Hemispheric Model with focus on intercontinental transport of air pollution, Atmos. Environ., 53, 156–176, doi:10.1016/j.atmosenv.2012.01.011, 2012. 6672, 6673, 6678

Christensen, J. H.: The Danish Eulerian Hemispheric Model – a three-dimensional air pollution model used for the Arctic, Atmos. Environ., 31, 4169–4191, 1997. 6672, 6678

Colette, A., Granier, C., Hodnebrog, Ø., Jakobs, H., Maurizi, A., Nyiri, A., Bessagnet, B., D'Angiola, A., D'Isidoro, M., Gauss, M., Meleux, F., Memmesheimer, M., Mieville, A., Rouïl, L., Russo, F., Solberg, S., Stordal, F., and Tampieri, F.: Air quality trends in Europe over the past decade: a first multi-model assessment, Atmos. Chem. Phys., 11, 11657–11678, doi:10.5194/acp-11-11657-2011, 2011. 6666

Colette, A., Granier, C., Hodnebrog, Ø., Jakobs, H., Maurizi, A., Nyiri, A., Rao, S., Amann, M., Bessagnet, B., D'Angiola, A., Gauss, M., Heyes, C., Klimont, Z., Meleux, F., Memmesheimer, M., Mieville, A., Rouïl, L., Russo, F., Schucht, S., Simpson, D., Stordal, F.,

ACPD
14, 6663–6720, 2014

Tampieri, F., and Vrac, M.: Future air quality in Europe: a multi-model assessment of projected exposure to ozone, Atmos. Chem. Phys., 12, 10613–10630, doi:10.5194/acp-12-10613-2012, 2012. 6666

Cuvelier, C., Thunis, P., Vautard, R., Amann, M., Bessagnet, B., Bedogni, M., Berkowicz, R., Brandt, J., Brocheton, F., Builtjes, P., Carnavale, C., Coppalle, A., Denby, B., Douros, J., Graf, A., Hellmuth, O., Hodzic, A., Honore, C., Jonson, J., Kerschbaumer, A., de Leeuw, F., Minguzzi, E., Moussiopoulos, N., Pertot, C., Peuch, V., Pirovano, G., Rouil, L., Sauter, F., Schaap, M., Stern, R., Tarrason, L., Vignati, E., Volta, M., White, L., Wind, P., and Zuber, A.: CityDelta: a model intercomparison study to explore the impact of emission reductions in European cities in 2010, Atmos. Environ., 41, 189–207, 2007. 6666

De Vries, W. and Posch, M.: Critical levels and critical loads as a tool for air quality management, in: Handbook of Atmospheric Science – Principles and Applications, edited by: Hewitt, C. N. and Jackson, A. V., chap. 20, Blackwell Science, Oxford, UK, 562–602, 2003. 6683

Dentener, F., Drevet, J., Lamarque, J. F., Bey, I., Eickhout, B., Fiore, A. M., Hauglustaine, D., Horowitz, L. W., Krol, M., Kulshrestha, U. C., Lawrence, M., Galy-Lacaux, C., Rast, S., Shindell, D., Stevenson, D., Van Noije, T., Atherton, C., Bell, N., Bergman, D., Butler, T., Cofala, J., Collins, B., Doherty, R., Ellingsen, K., Galloway, J., Gauss, M., Montanaro, V., Mueller, J. F., Pitari, G., Rodriguez, J., Sanderson, M., Solmon, F., Strahan, S., Schultz, M., Sudo, K., Szopa, S., and Wild, O.: Nitrogen and sulfur deposition on regional and global scales: a multimodel evaluation, Global Biogeochem. Cy., 20, GB4003, doi:10.1029/2005GB002672, 2006. 6666, 6682

Dore, A., Carslaw, D., Chemel, C., Derwent, R., Fisher, B., Griffiths, S., Lawrence, S., Metcalfe, S., Redington, A., Simpson, D., Sokhi, R., Sutton, P., Vieno, M., and Whyatt, J.: Evaluation and inter-comparison of AIC deposition models for the UK, in: Air Pollution Modelling and its Application XXII, edited by: Steyn, D., Builtjes, P., and Timmermans, R., NATO Science for Peace and Security Series C. Environmental Security, Springer, Dordrecht, 32nd NATO/SPS International Technical Meeting, 505–509, 2013. 6666, 6674

Emberson, L., Simpson, D., Tuovinen, J.-P., Ashmore, M., and Cambridge, H.: Towards a model of ozone deposition and stomatal uptake over Europe, EMEP MSC-W Note 6/2000, The Norwegian Meteorological Institute, Oslo, Norway, 2000a. 6673

Emberson, L., Wieser, G., and Ashmore, M.: Modelling of stomatal conductance and ozone flux of Norway spruce: comparison with field data, Environ. Pollut., 109, 393–402, 2000b. 6673

ACPD
14, 6663–6720, 2014

Emberson, L., Ashmore, M., Simpson, D., Tuovinen, J.-P., and Cambridge, H.: Modelling and mapping ozone deposition in Europe, Water Air Soil Pollut., 130, 577–582, 2001. 6673
Emberson, L. D., Büker, P., and Ashmore, M. R.: Assessing the risk caused by ground level ozone to European forest trees: a case study in pine, beech and oak across different climate regions, Environ. Pollut., 147, 454–466, doi:10.1016/j.envpol.2006.10.026, 2007. 6673
Engardt, M.: Sulphur simulations for East Asia using the MATCH model with meteorological data from ECMWF, RMK 88, Swedish Meteorological and Hydrological Institute, 33 pp., 2000. 6675
Engardt, M. and Langner, J.: Simulations of future sulphur and nitrogen deposition over Europe using meteorological data from three regional climate projections, Tellus B, 65, 20348, doi:10.3402/tellusb.v65i0.20348, 2013. 6665, 6666, 6675, 6681
Erisman, J. W., Hensen, A., Fowler, D., Flechard, C. R., Grüner, A., Spindler, G., Duyzer, J. H., Weststrate, H., Römer, F., Vonk, A. W., and Jaarsveld, H. V.: Dry deposition monitoring in Europe, Water Air Soil Pollut., 1, 17–27, 2001. 6674
Erisman, J. W., Galloway, J. N., Seitzinger, S., Bleeker, A., Dise, N. B., Petrescu, A. M. R., Leach, A. M., and de Vries, W.: Consequences of human modification of the global nitrogen cycle, Philos.Trans. R. Soc. Lond. B. Biol. Sci., 368, doi:10.1098/rstb.2013.0116, 2013. 6665
Fagerli, H. and Aas, W.: Trends of nitrogen in air and precipitation: model results and observations at EMEP sites in Europe, 1980–2003, Environ. Pollut., 154, 448–461, 2008. 6674
Finlayson-Pitts, B. and Pitts, J.: Chemistry of the Upper and Lower Atmosphere – Theory, Experiments, and Applications, Academic Press, San Diego, CA, USA, 2000. 6676
Flechard, C. R., Nemitz, E., Smith, R. I., Fowler, D., Vermeulen, A. T., Bleeker, A., Erisman, J. W., Simpson, D., Zhang, L., Tang, Y. S., and Sutton, M. A.: Dry deposition of reactive nitrogen to European ecosystems: a comparison of inferential models across the NitroEurope network, Atmos. Chem. Phys., 11, 2703–2728, doi:10.5194/acp-11-2703-2011, 2011. 6685
Flechard, C. R., Massad, R.-S., Loubet, B., Personne, E., Simpson, D., Bash, J. O., Cooter, E. J., Nemitz, E., and Sutton, M. A.: Advances in understanding, models and parameterizations of biosphere-atmosphere ammonia exchange, Biogeosciences, 10, 5183–5225, doi:10.5194/bg-10-5183-2013, 2013. 6682, 6686
Forkel, R. and Knoche, R.: Nested regional climate-chemistry simulations for central Europe, C. R. Geosci., 339, 734–746, doi:10.1016/j.crte.2007.09.018, 2007. 6665

ACPD
14, 6663–6720, 2014

Fowler, D. and Erisman, J.: Biosphere/atmosphere exchange of pollutants, overview of subproject BIATEX-2, in: Towards Cleaner Air for Europe – Science, Tools and Applications, Part 2. Overviews from the Final Reports of the EUROTRAC-2 Subprojects, edited by: Midgley, P. and Reuther, M., Margraf Verlag, Weikersheim, also available at: http://www.gsf.de/eurotrac/publications/ (last access: 22 February 2014) , 2003. 6674

Fowler, D., Pilegaard, K., Sutton, M., Ambus, P., Raivonen, M., Duyzer, J., Simpson, D., Fagerli, H., Fuzzi, S., Schjoerring, J., Granier, C., Neftel, A., Isaksen, I., Laj, P., Maione, M., Monks, P., Burkhardt, J., Daemmgen, U., Neirynck, J., Personne, E., Wichink-Kruit, R., Butterbach-Bahl, K., Flechard, C., Tuovinen, J., Coyle, M., Gerosa, G., Loubet, B., Altimir, N., Gruenhage, L., Ammann, C., Cieslik, S., Paoletti, E., Mikkelsen, T., Ro-Poulsen, H., Cellier, P., Cape, J., Horváth, L., Loreto, F., Niinemets, Ü., Palmer, P., Rinne, J., Misztal, P., Nemitz, E., Nilsson, D., Pryor, S., Gallagher, M., Vesala, T., Skiba, U., Brüeggemann, N., Zechmeister-Boltenstern, S., Williams, J., O'Dowd, C., Facchini, M., de Leeuw, G., Flossman, A., Chaumerliac, N., and Erisman, J.: Atmospheric composition change: ecosystems–atmosphere interactions, Atmos. Environ., 43, 5193–5267, doi:10.1016/j.atmosenv.2009.07.068, 2009. 6674, 6685, 6686

Frohn, L., Christensen, J., and Brandt, J.: Development and testing of numerical methods for two-way nested air pollution modelling, Phys. Chem. Earth, 27, 1487–1494, doi:10.1016/S1474-7065(02)00151-1, 2002. 6672

Gallagher, M. W., Beswick, K. M., Duyzer, J., Westrate, H., Choularton, T. W., and Hummelshoj, P.: Measurements of aerosol fluxes to Speulder forest using a micrometeorological technique, Atmos. Environ., 31, 359–373, 1997. 6674

Geels, C., Brandt, J., Christensen, J., Frohn, L., and Hansen, K.: Long-term calculations with a comprehensive nested hemispheric air pollution transport model, in: Advances in Air Pollution Modeling for Environmental Security, edited by: Faragó, I., Georgiev, K., and Havasi, Á., Springer, Netherlands, 185–196, 2005. 6673, 6678

Geels, C., Andersen, H. V., Ambelas Skjøth, C., Christensen, J. H., Ellermann, T., Løfstrøm, P., Gyldenkærne, S., Brandt, J., Hansen, K. M., Frohn, L. M., and Hertel, O.: Improved modelling of atmospheric ammonia over Denmark using the coupled modelling system DAMOS, Biogeosciences, 9, 2625–2647, doi:10.5194/bg-9-2625-2012, 2012a. 6672

Geels, C., Hansen, K. M., Christensen, J. H., Ambelas Skjøth, C., Ellermann, T., Hedegaard, G. B., Hertel, O., Frohn, L. M., Gross, A., and Brandt, J.: Projected change in at-

ACPD
14, 6663–6720, 2014

mospheric nitrogen deposition to the Baltic Sea towards 2020, Atmos. Chem. Phys., 12, 2615–2629, doi:10.5194/acp-12-2615-2012, 2012b. 6666, 6673
Guenther, A., Hewitt, C., Erickson, D., Fall, R., Geron, C., Graedel, T., Harley, P., Klinger, L., Lerdau, M., McKay, W., Pierce, T., Scholes, R., Steinbrecher, R., Tallamraju, R., Taylor, J., and Zimmerman, P.: A global model of natural volatile organic compound emissions, J. Geophys. Res., 100, 8873–8892, doi:10.1029/94JD02950, 1995. 6673
Hedegaard, G. B., Brandt, J., Christensen, J. H., Frohn, L. M., Geels, C., Hansen, K. M., and Stendel, M.: Impacts of climate change on air pollution levels in the Northern Hemisphere with special focus on Europe and the Arctic, Atmos. Chem. Phys., 8, 3337–3367, doi:10.5194/acp-8-3337-2008, 2008. 6665, 6678
Hedegaard, G. B., Christensen, J. H., and Brandt, J.: The relative importance of impacts from climate change vs. emissions change on air pollution levels in the 21st century, Atmos. Chem. Phys., 13, 3569–3585, doi:10.5194/acp-13-3569-2013, 2013. 6666
Hertel, O., Christensen, J., Runge, E., Asman, W., Berkowicz, R., Hovmand, M., and Hov, O.: Development and testing of a new variable scale air-pollution model – ACDEP, Atmos. Environ., 29, 1267–1290, 1995. 6673
Hettelingh, J., Posch, M., DeSmet, P. A. M., and Downing, J. R.: The use of critical loads in emission reduction agreements in Europe, Water Air Soil Pollut., 85, 2381–2388, doi:10.1007/BF01186190, 1995. 6683
Hettelingh, J.-P., Posch, M., and de Smet, P. A. M.: Multi-effect critical loads used in multi-pollutant reduction agreements in Europe, Water Air Soil Pollut., 130, 1133–1138, 2001. 6683
Hijioka, Y., Matsuoka, Y., Nishimoto, H., Masui, M., and Kainuma, M.: Global GHG emissions scenarios under GHG concentration stabilization targets, Journal of Global Environmental Engineering, 13, 97–108, 2008. 6669
Hole, L. and Engardt, M.: Climate change impact on atmospheric nitrogen deposition in northwestern Europe: a model study, Ambio, 37, 9–17, 2008. 6666
Hole, L. R., Christensen, J. H., Ruoho-Airola, T., Torseth, K., Ginzburg, V., and Glowacki, P.: Past and future trends in concentrations of sulphur and nitrogen compounds in the Arctic, Atmos. Environ., 43, 928–939, doi:10.1016/j.atmosenv.2008.10.043, 2009. 6665, 6666
Horn, H., Bonka, H., and Maqua, M.: Measured particle bound activity size-distribution, deposition velocity, and activity concentration in rainwater after the Chernobyl accident, J. Aerosol Sci., 18, 681–684, doi:10.1016/0021-8502(87)90096-6, 1987. 6676

ACPD
14, 6663–6720, 2014

Huijnen, V., Eskes, H. J., Poupkou, A., Elbern, H., Boersma, K. F., Foret, G., Sofiev, M., Valdebenito, A., Flemming, J., Stein, O., Gross, A., Robertson, L., D'Isidoro, M., Kioutsioukis, I., Friese, E., Amstrup, B., Bergstrom, R., Strunk, A., Vira, J., Zyryanov, D., Maurizi, A., Melas, D., Peuch, V.-H., and Zerefos, C.: Comparison of OMI NO_2 tropospheric columns with an ensemble of global and European regional air quality models, Atmos. Chem. Phys., 10, 3273–3296, doi:10.5194/acp-10-3273-2010, 2010. 6675

John, J. G., Fiore, A. M., Naik, V., Horowitz, L. W., and Dunne, J. P.: Climate versus emission drivers of methane lifetime against loss by tropospheric OH from 1860–2100, Atmos. Chem. Phys., 12, 12021–12036, doi:10.5194/acp-12-12021-2012, 2012. 6673

Jylhä, K.: Empirical scavenging coefficients of radioactive substances released from Chernobyl, Atmos. Environ. A-Gen., 25, 263–270, doi:10.1016/0960-1686(91)90297-K, 1991. 6676

Kjellstrom, E., Nikulin, G., Hansson, U., Strandberg, G., and Ullerstig, A.: 21st century changes in the European climate: uncertainties derived from an ensemble of regional climate model simulations, Tellus A, 63, 24–40, doi:10.1111/j.1600-0870.2010.00475.x, 2011. 6671

Klingberg, J., Danielsson, H., Simpson, D., and Pleijel, H.: Comparison of modelled and measured ozone concentrations and meteorology for a site in south-west Sweden: implications for ozone uptake calculations, Environ. Pollut., 115, 99–111, 2008. 6673

Kouznetsov, R. and Sofiev, M.: A methodology for evaluation of vertical dispersion and dry deposition of atmospheric aerosols, J. Geophys. Res., 117, D01202doi:10.1029/2011JD016366, 2012. 6676

Kuenen, J., Denier van der Gon, H., Visschedijk, A., van der Brugh, H., and van Gijlswijk, R.: MACC European emission inventory for the years 2003–2007, TNO Report TNO-060-UT-2011-00588, TNO, Utrecht, the Netherlands, 2011. 6669

Kukkonen, J., Olsson, T., Schultz, D. M., Baklanov, A., Klein, T., Miranda, A. I., Monteiro, A., Hirtl, M., Tarvainen, V., Boy, M., Peuch, V.-H., Poupkou, A., Kioutsioukis, I., Finardi, S., Sofiev, M., Sokhi, R., Lehtinen, K. E. J., Karatzas, K., San José, R., Astitha, M., Kallos, G., Schaap, M., Reimer, E., Jakobs, H., and Eben, K.: A review of operational, regional-scale, chemical weather forecasting models in Europe, Atmos. Chem. Phys., 12, 1–87, doi:10.5194/acp-12-1-2012, 2012. 6675

Lamarque, J., Kiehl, J., Brasseur, G., Butler, T., Cameron-Smith, P., Collins, W., Collins, W., Granier, C., Hauglustaine, D., Hess, P., Holland, E., Horowitz, L., Lawrence, M., McKenna, D., Merilees, P., Prather, M., Rasch, P., Rotman, D., Shindell, D., and Thornton, P.: Assessing future nitrogen deposition and carbon cycle feedback using a multimodel approach: analysis

ACPD
14, 6663–6720, 2014

of nitrogen deposition, J. Geophys. Res., 110, D19303, doi:10.1029/2005JD005825, 2005. 6666, 6682
Lamaud, E., Brunet, Y., Labatut, A., Lopez, A., Fontan, J., and Druilhet, A.: The Landes experiment: biosphere–atmosphere exchanges of ozone and aerosol particles above a pine forest, J. Geophys. Res., 99, 16511–16521, doi:10.1029/94JD00668, 1994. 6674
Langner, J., Bergström, R., and Pleijel, K.: European scale modeling of sulfur, oxidised nitrogen and photochemical oxidants, Model development and evaluation for the 1994 growing season, RMK No. 82, Swedish Meteorological and Hydrological Institute, (with errata), Norrköping, Sweden, 1998. 6675
Langner, J., Bergstrom, R., and Foltescu, V.: Impact of climate change on surface ozone and deposition of sulphur and nitrogen in Europe, Atmos. Environ., 39, 1129–1141, doi:10.1016/j.atmosenv.2004.09.082, 2005. 6665
Langner, J., Andersson, C., and Engardt, M.: Atmospheric input of nitrogen to the Baltic sea basin: present situation, variability due to meteorology and impact of climate change, Boreal Environ. Res., 14, 226–237, 2009. 6666, 6675
Langner, J., Engardt, M., and Andersson, C.: European summer surface ozone 1990–2100, Atmos. Chem. Phys., 12, 10097–10105, doi:10.5194/acp-12-10097-2012, 2012a. 6665
Langner, J., Engardt, M., Baklanov, A., Christensen, J. H., Gauss, M., Geels, C., Hedegaard, G. B., Nuterman, R., Simpson, D., Soares, J., Sofiev, M., Wind, P., and Zakey, A.: A multi-model study of impacts of climate change on surface ozone in Europe, Atmos. Chem. Phys., 12, 10423–10440, doi:10.5194/acp-12-10423-2012, 2012b. 6665, 6666, 6667, 6669, 6671, 6672
Loubet, B., Milford, C., Sutton, M. A., and Cellier, P.: Investigation of the interaction between sources and sinks of atmospheric ammonia in an upland landscape using a simplified dispersion-exchange model, J. Geophys. Res., 106, 24183–24195, 2001. 6687
Loubet, B., Asman, W. A., Theobald, M. R., Hertel, O., Tang, Y. S., Robin, P., Hassouna, M., Dämmgen, U., Genermont, S., Cellier, P., and Sutton, M. A.: Ammonia deposition near hot spots: processes, models and monitoring methods, in: Atmospheric Ammonia, Detecting Emissions Changes and Environmental Impacts, edited by: Sutton, M. A., Reis, S., and Baker, S. M., Springer, 205–267, Dordrecht, Netherlands, 2009. 6687
Massad, R.-S., Nemitz, E., and Sutton, M. A.: Review and parameterisation of bi-directional ammonia exchange between vegetation and the atmosphere, Atmos. Chem. Phys., 10, 10359–10386, doi:10.5194/acp-10-10359-2010, 2010. 6686

ACPD
14, 6663–6720, 2014

Nakićenović, N.: Global greenhouse gas emissions scenarios: integrated modeling approaches, Technol. Forecast. Soc., 63, 105–109, 2000. 6671

Nemitz, E. and Sutton, M. A.: Gas-particle interactions above a Dutch heathland: III. Modelling the influence of the NH_3-HNO_3-NH_4NO_3 equilibrium on size-segregated particle fluxes, Atmos. Chem. Phys., 4, 1025–1045, doi:10.5194/acp-4-1025-2004, 2004. 6686

Nemitz, E., Sutton, M. A., Wyers, G. P., Otjes, R. P., Mennen, M. G., van Putten, E. M., and Gallagher, M. W.: Gas-particle interactions above a Dutch heathland: II. Concentrations and surface exchange fluxes of atmospheric particles, Atmos. Chem. Phys., 4, 1007–1024, doi:10.5194/acp-4-1007-2004, 2004. 6674

Nilsson, J. and Grennfelt, P. (eds.): Critical Loads for Sulphur and Nitrogen, Nord 1988:97, Nordic Council of Ministers, Copenhagen, Denmark, Nord 1988:97, 418 pp., 1988. 6682

Posch, M., DeSmet, P. A. M., Hettelingh, J.-P., and Downing, J. R. (Eds.): Modelling and mapping of critical thresholds in Europe, Status report 2001, Coordination Centre for Effects, RIVM, Bilthoven, the Netherlands, 2001. 6684

Posch, M., Slootweg, J., and Hettelingh, J. (eds.): Modelling critical thresholds and temporal changes of geochemistry and vegetation diversity, CCE Status Report 2011, 680359003, RIVM, Bilthoven, the Netherlands, available at: www.wge-cce.org (last access: 2 February 2014), 2011. 6683

Posch, M., Slootweg, J., and Hettelingh, J. (eds.): Modelling and mapping of atmospherically-induced ecosystem impacts in Europe: CCE Status Report 2012, 680359004, RIVM, Bilthoven, the Netherlands, available at: www.wge-cce.org (last access: 2 February 2014), 2012. 6683

Pryor, S. C., Gallagher, M., Sievering, H., Larsen, S. E., Barthelmie, R. J., Birsan, F., Nemitz, E., Rinne, J., Kulmala, M., Groenholm, T., Taipale, R., and Vesala, T.: A review of measurement and modelling results of particle atmosphere-surface exchange, Tellus, 60, 42–75, doi:10.1111/j.1600-0889.2007.00298.x, 2008. 6685

Reis, S., Grennfelt, P., Klimont, Z., Amann, M., ApSimon, H., Hettelingh, J.-P., Holland, M., LeGall, A.-C., Maas, R., Posch, M., Spranger, T., Sutton, M. A., and Williams, M.: From acid rain to climate change, Science, 338, 1153–1154, doi:10.1126/science.1226514, 2012. 6683

Robertson, L., Langner, J., and Engardt, M.: An Eulerian limited-area atmospheric transport model, J. Appl. Meteorol., 38, 190–210, 1999. 6675, 6677

Roeckner, E., Brokopf, R., Esch, M., Giorgetta, M., Hagemann, S., Kornblueh, L., Manzini, E., Schlese, U., and Schulzweida, U.: Sensitivity of simulated climate to horizontal and

ACPD
14, 6663–6720, 2014

vertical resolution in the ECHAM5 atmosphere model, J. Climate, 19, 3771–3791, doi:10.1175/JCLI3824.1, 2006. 6671
Samuelsson, P., Jones, C. G., Willen, U., Ullerstig, A., Gollvik, S., Hansson, U., Jansson, C., Kjellstrom, E., Nikulin, G., and Wyser, K.: The Rossby Centre Regional Climate model RCA3: model description and performance, Tellus A, 63, 4–23, doi:10.1111/j.1600-0870.2010.00478.x, 2011. 6671
Sanderson, M., Dentener, F., Fiore, A., Cuvelier, K., Keating, T., Zuber, A., Atherton, C., Bergmann, D., Diehl, T., Doherty, R., Duncan, B., Hess, P., Horowitz, L., Jacob, D., Jonson, J., Kaminski, J., Lupu, A., Mackenzie, I., Mancini, E., Marmer, E., Park, R., Pitari, G., Prather, M., Pringle, K., Schroeder, S., Schultz, M., Shindell, D., Szopa, S., Wild, O., and Wind, P.: A multi-model study of the hemispheric transport and deposition of oxidised nitrogen, Geophys. Res. Lett., 35, L17815, doi:10.1029/2008GL035389, 2008. 6666
Simpson, D., Andersson-Sköld, Y., and Jenkin, M. E.: Updating the chemical scheme for the EMEP MSC-W oxidant model: current status, EMEP MSC-W Note 2/93, The Norwegian Meteorological Institute, Oslo, Norway, 1993. 6675
Simpson, D., Winiwarter, W., Börjesson, G., Cinderby, S., Ferreiro, A., Guenther, A., Hewitt, C. N., Janson, R., Khalil, M. A. K., Owen, S., Pierce, T. E., Puxbaum, H., Shearer, M., Skiba, U., Steinbrecher, R., Tarrasón, L., and Öquist, M. G.: Inventorying emissions from nature in Europe, J. Geophys. Res., 104, 8113–8152, 1999. 6669
Simpson, D., Tuovinen, J.-P., Emberson, L., and Ashmore, M.: Characteristics of an ozone deposition module, Water Air Soil Pollut., 1, 253–262, 2001. 6673
Simpson, D., Fagerli, H., Jonson, J., Tsyro, S., Wind, P., and Tuovinen, J.-P.: The EMEP Unified Eulerian Model, Model Description, EMEP MSC-W Report 1/2003, The Norwegian Meteorological Institute, Oslo, Norway, 2003a. 6673
Simpson, D., Tuovinen, J.-P., Emberson, L., and Ashmore, M.: Characteristics of an ozone deposition module II: sensitivity analysis, Water Air Soil Pollut., 143, 123–137, 2003b. 6673
Simpson, D., Butterbach-Bahl, K., Fagerli, H., Kesik, M., Skiba, U., and Tang, S.: Deposition and emissions of reactive nitrogen over European forests: a modelling study, Atmos. Environ., 40, 5712–5726, doi:10.1016/j.atmosenv.2006.04.063, 2006a. 6674
Simpson, D., Fagerli, H., Hellsten, S., Knulst, J. C., and Westling, O.: Comparison of modelled and monitored deposition fluxes of sulphur and nitrogen to ICP-forest sites in Europe, Biogeosciences, 3, 337–355, doi:10.5194/bg-3-337-2006, 2006b. 6674

ACPD
14, 6663–6720, 2014

Simpson, D., Benedictow, A., Berge, H., Bergström, R., Emberson, L. D., Fagerli, H., Flechard, C. R., Hayman, G. D., Gauss, M., Jonson, J. E., Jenkin, M. E., Nyíri, A., Richter, C., Semeena, V. S., Tsyro, S., Tuovinen, J.-P., Valdebenito, Á., and Wind, P.: The EMEP MSC-W chemical transport model – technical description, Atmos. Chem. Phys., 12, 7825–7865, doi:10.5194/acp-12-7825-2012, 2012. 6673, 6674, 6677

Skjøth, C. A. and Geels, C.: The effect of climate and climate change on ammonia emissions in Europe, Atmos. Chem. Phys., 13, 117–128, doi:10.5194/acp-13-117-2013, 2013. 6665, 6668, 6670

Skjøth, C. A., Geels, C., Berge, H., Gyldenkærne, S., Fagerli, H., Ellermann, T., Frohn, L. M., Christensen, J., Hansen, K. M., Hansen, K., and Hertel, O.: Spatial and temporal variations in ammonia emissions – a freely accessible model code for Europe, Atmos. Chem. Phys., 11, 5221–5236, doi:10.5194/acp-11-5221-2011, 2011. 6670

Smith, F. B. and Clark, M. J.: The transport and deposition of radioactive debris from the Chernobyl nuclear power plant accident with special emphasis on consequences to the UK, Meteorological Office Scientific Paper N42, Meteorological Office Scientific Paper, HMSO, London, 1989. 6676

Sofiev, M.: A model for the evaluation of long-term airborne pollution transport at regional and continental scales, Atmos. Environ., 34, 2481–2493, 2000. 6676

Sofiev, M., Siljamo, P., Valkama, I., Ilvonen, M., and Kukkonen, J.: A dispersion modelling system SILAM and its evaluation against ETEX data, Atmos. Environ., 40, 674–685, doi:10.1016/j.atmosenv.2005.09.069, 2006. 6676

Sofiev, M., Galperin, M., and Genikhovich, E.: A construction and evaluation of Eulerian dynamic core for the air quality and emergency modelling system SILAM, in: Air Pollution Modeling and its Application XIX, edited by: Borrego, C. and Miranda, A. I., Nato Science for Peace and Security Series C – Environmental Security, NATO; CCMS; Univ Aveiro, doi:10.1007/978-1-4020-8453-9_94, 699–701, 2008. 6675

Sofiev, M., Genikhovich, E., Keronen, P., and Vesala, T.: Diagnosing the surface layer parameters for dispersion models within the meteorological-to-dispersion modeling interface, J. Appl. Meteorol. Clim., 49, 221–233, doi:10.1175/2009JAMC2210.1, 2010. 6676

Solazzo, E., Bianconi, R., Vautard, R., Appel, K. W., Moran, M. D., Hogrefe, C., Bessagnet, B., Brandt, J., Christensen, J. H., Chemel, C., Coll, I., van der Gon, H. D., Ferreira, J., Forkel, R., Francis, X. V., Grell, G., Grossi, P., Hansen, A. B., Jericevic, A., Kraljevic, L., Miranda, A. I., Nopmongcol, U., Pirovano, G., Prank, M., Riccio, A., Sartelet, K. N., Schaap, M.,

ACPD
14, 6663–6720, 2014

Silver, J. D., Sokhi, R. S., Vira, J., Werhahn, J., Wolke, R., Yarwood, G., Zhang, J., Rao, S. T., and Galmarini, S.: Model evaluation and ensemble modelling of surface-level ozone in Europe and North America in the context of AQMEII, Atmos. Environ., 53, 60–74, doi:10.1016/j.atmosenv.2012.01.003, 2012. 6666

Strand, A. and Hov, O.: A 2-dimensional global study of tropospheric ozone production, J. Geophys. Res., 99, 22877–22895, doi:10.1029/94JD01945, 1994. 6673

Sutton, M., Schjorring, J., and Wyers, G.: Plant atmosphere exchange of ammonia, Philos. T. Roy. Soc. Lond. A, 351, 261–276, 1995. 6686

Sutton, M., Howard, C., Erisman, J., Billen, G., Bleeker, A., Grennfelt, P., van Grinsven, H., and Grizetti, B. (eds.): The European Nitrogen Assessment, Sources, Effects and Policy Perspectives, Cambridge University Press, New York, 2011. 6665

Sutton, M. A., Reis, S., Riddick, S. N., Dragosits, U., Nemitz, E., Theobald, M. R., Tang, Y. S., Braban, C. F., Vieno, M., Dore, A. J., Mitchell, R. F., Wanless, S., Daunt, F., Fowler, D., Blackall, T. D., Milford, C., Flechard, C. R., Loubet, B., Massad, R., Cellier, P., Personne, E., Coheur, P. F., Clarisse, L., Van Damme, M., Ngadi, Y., Clerbaux, C., Skjøth, C. A., Geels, C., Hertel, O., Wichink Kruit, R. J., Pinder, R. W., Bash, J. O., Walker, J. T., Simpson, D., Horváth, L., Misselbrook, T. H., Bleeker, A., Dentener, F., and de Vries, W.: Towards a climate-dependent paradigm of ammonia emission and deposition, Philos. T. Roy. Soc. B, 368, 1621 20130166, doi:10.1098/rstb.2013.0166, 2013. 6665, 6668, 6670

Thunis, P., Rouil, L., Cuvelier, C., Stern, R., Kerschbaumer, A., Bessagnet, B., Schaap, M., Builtjes, P., Tarrason, L., Douros, J., Moussiopoulos, N., Pirovano, G., and Bedogni, M.: Analysis of model responses to emission-reduction scenarios within the CityDelta project, Atmos. Environ., 41, 208–220, 2007. 6666

Tørseth, K., Aas, W., Breivik, K., Fjæraa, A. M., Fiebig, M., Hjellbrekke, A. G., Lund Myhre, C., Solberg, S., and Yttri, K. E.: Introduction to the European Monitoring and Evaluation Programme (EMEP) and observed atmospheric composition change during 1972–2009, Atmos. Chem. Phys., 12, 5447–5481, doi:10.5194/acp-12-5447-2012, 2012. 6677

Tuovinen, J.-P., Simpson, D., Mikkelsen, T. N., Emberson, L. D., Ashmore, M. R., Aurela, M., Cambridge, H. M., Hovmand, M. F., Jensen, N. O., Laurila, T., Pilegaard, K., and Ro-Poulsen, H.: Comparisons of measured and modelled ozone deposition to forests in Northern Europe, Water Air Soil Pollut., 1, 263–274, 2001. 6673

Tuovinen, J.-P., Ashmore, M., Emberson, L., and Simpson, D.: Testing and improving the EMEP ozone deposition module, Atmos. Environ., 38, 2373–2385, 2004. 6673

ACPD
14, 6663–6720, 2014

Tuovinen, J.-P., Hakola, H., Karlsson, P. E., and Simpson, D.: Air pollution risks to Northern European forests in a changing climate, in: Climate Change, Air Pollution and Global Challenges Understanding and Perspectives from Forest Research, edited by: Matyssek, R., Clarke, N., Cudlin, P., Mikkelsen, T., Tuovinen, J., Wieser, G., and Paoletti, E., vol. 13 of Developments in Environmental Science, chap. 5, Elsevier, doi:10.1016/B978-0-08-098349-3.00005-0, Oxford, UK, 77–99, 2013. 6666

UNECE: Manual on methodologies and criteria for modelling and mapping critical loads and levels, and air pollution effects, risks and trends, Tech. rep., UNECE Convention on Long-range Transboundary Air Pollution, available at: www.icpmapping.org (last access: 22 February 2014), 2004. 6683

van der Linden, P. and Mitchell, J. F. B.: ENSEMBLES: Climate Change and its Impacts: Summary of research and results from the ENSEMBLES project, Tech. rep., Met Office Hadley Centre, FitzRoy Road, Exeter EX1 3PB, UK, available at: http://ensembles-eu.metoffice.com/docs/Ensembles_final_report_Nov09.pdf, 2009. 6670

van Loon, M., Vautard, R., Schaap, M., Bergstrom, R., Bessagnet, B., Brandt, J., Builtjes, P., Christensen, J., Cuvelier, C., Graff, A., Jonson, J., Krol, M., Langner, J., Roberts, P., Rouil, L., Stern, R., Tarrason, L., Thunis, P., Vignati, E., White, L., and Wind, P.: Evaluation of long-term ozone simulations from seven regional air quality models and their ensemble, Atmos. Environ., 41, 2083–2097, 2007. 6666

Vautard, R., Van Loon, M., Schaap, M., Bergstroem, R., Bessagnet, B., Brandt, J., Builtjes, P. J. H., Christensen, J. H., Cuvelier, C., Graff, A., Jonson, J. E., Krol, M., Langner, J., Roberts, P., Rouil, L., Stern, R., Tarrason, L., Thunis, P., Vignati, E., White, L., and Wind, P.: Is regional air quality model diversity representative of uncertainty for ozone simulation?, Geophys. Res. Lett., 33, L24818, doi:10.1029/2006GL027610, 2006. 6666

Vautard, R., Builtjes, P., Thunis, P., Cuvelier, C., Bedogni, M., Bessagnet, B., Honore, C., Moussiopoulos, N., Pirovano, G., Schaap, M., Stern, R., Tarrason, L., and Wind, P.: Evaluation and intercomparison of ozone and PM_{10} simulations by several chemistry transport models over four European cities within the CityDelta project, Atmos. Environ., 41, 173–188, doi:10.1016/j.atmosenv.2006.07.039, 2007. 6666

Wesely, M. L., Cook, D. R., Hart, R. L., and Speer, R. E.: Measurements and parameterization of particulate sulfur dry deposition over grass, J. Geophys. Res., 90, 2131–2143, 1985. 6674

ACPD
14, 6663–6720, 2014

Wichink-Kruit, R., van Pul, W., Sauter, F., van den Broek, M., Nemitz, E., Sutton, M., Krol, M., and Holtslag, A.: Modeling the surface–atmosphere exchange of ammonia, Atmos. Environ., 44, 945–957, doi:10.1016/j.atmosenv.2009.11.049, 2010. 6682, 6686

Wichink Kruit, R. J., Schaap, M., Sauter, F. J., van Zanten, M. C., and van Pul, W. A. J.: Modeling the distribution of ammonia across Europe including bi-directional surface–atmosphere exchange, Biogeosciences, 9, 5261–5277, doi:10.5194/bg-9-5261-2012, 2012. 6686

ACPD

14, 6663–6720, 2014

Table 1. Model runs used in this study.

Label	Emis.	Meteor.	BIC label	DEHM-setup	Comment
E05-M00-BC1	2005	1990–2009	BC1	E05-M00	Base-case – current conditions
E05-M50-BC2	2005	2040–2059	BC2	E05-M50	Climate change only
E05-M50-BC3	2005	2040–2059	BC3	E50-M50	Climate+boundary condition changes
E50-M50-BC3	2050	2040–2059	BC3	E50-M50	Future conditions
E50X20-M50-BC3	2050	2040–2059	BC3	E50-M50	20 % more NH_3, EMEP, DEHM only
E50X30-M50-BC3	2050	2040–2059	BC3	E50-M50	30 % more NH_3, EMEP only

ACPD
14, 6663–6720, 2014

Table 2. Emissions for EU28^{+} used in the calculations for 2005 and 2050. Units: Tg yr^{-1} (SO_x as SO_2, NO_x as NO_2).

Year	SO_x	NO_x	NH_3	NMVOC
2005	8.41	12.5	3.99	10.1
2050	2.10	4.10	4.04	5.94
Change (%)	−75	−67	+1	−41

Notes: EU28^{+} here denotes the 28 EU countries, plus Norway and Switzerland.

ACPD
14, 6663–6720, 2014

Table 3. Evaluation of modelled air concentrations of sulphur and nitrogen gaseous and aerosol species using observations from the EMEP measurement network (http://www.emep.int) for the years 2000–2010. Unit: $\mu g(S/N)m^{-3}$.

	SO_2	NO_2	NH_3	HNO_3	SO_4^{2-}-tot	SO_4^{2-}-nss	$NH_3 + NH_4^+$	$HNO_3 + NO_3$
OBS	0.76	2.1	1.2	0.14	0.66	0.44	1.3	0.51
MOD-DEHM	0.83	2.0	0.9	0.23	0.91	0.59	2.2	1.1
MOD-EMEP	0.68	1.9	0.7	0.11	0.58	0.39	1.1	0.53
MOD-MATCH	0.68	1.8	0.5	0.09	0.79	0.54	1.0	0.34
MOD-SILAM	0.58	2.6	0.8	0.12	0.29	0.19	1.6	1.00
bias-DEHM (%)	9	−6	−26	67	37	33	62	111
bias-EMEP (%)	−11	−9	−46	−16	−12	−12	−14	4
bias-MATCH (%)	−10	−14	−62	−30	18	21	−24	−32
bias-SILAM (%)	−24	25	−34	−14	−55	−57	20	94
R-DEHM	0.67	0.74	0.85	0.34	0.69	0.97	0.74	0.80
R-EMEP	0.62	0.84	0.90	0.48	0.78	0.96	0.79	0.82
R-MATCH	0.55	0.84	0.88	0.46	0.71	0.84	0.75	0.75
R-SILAM	0.50	0.81	0.91	0.51	0.76	0.95	0.76	0.81
RMSE-DEHM	0.58	1.0	1.1	0.20	0.42	0.20	1.2	0.68
RMSE-EMEP	0.63	0.83	1.2	0.15	0.22	0.09	0.55	0.17
RMSE-MATCH	0.67	0.92	1.5	0.15	0.35	0.25	0.63	0.26
RMSE-SILAM	0.76	1.1	1.1	0.15	0.43	0.30	0.7	0.59
stns	85	85	18	16	65	16	49	49

Notes: SO_4^{2-}-tot and SO_4^{2-}-nss means total and sea-salt corrected sulphate, respectively.

ACPD
14, 6663–6720, 2014

Table 4. Evaluation of modelled wet deposition, concentration in precipitation (C_p) and precipitation using observations from the EMEP measurement network for the years 2000–2010.

	Deposition kg(N/S) ha^{-1}			C_p mg(S/N) L^{-1}			Precip. (mm)
	SO_x	NO_y	NH_x	SO_x	NO_y	NH_x	
OBS	3.10	2.82	3.34	0.39	0.34	0.40	878
MOD-DEHM	3.25	3.00	3.04	0.45	0.45	0.41	770
MOD-EMEP	4.18	2.90	3.54	0.40	0.40	0.33	1119
MOD-MATCH	5.64	3.52	4.07	0.53	0.34	0.37	1119
MOD-SILAM	2.39	4.85	3.92	0.22	0.22	0.35	1119
bias-DEHM (%)	4	6	−8	15	32	2	−12
bias-EMEP (%)	35	2	6	2	15	−16	27
bias-MATCH (%)	82	24	21	33	−1	−5	27
bias-SILAM (%)	−22	72	17	−43	−35	−10	27
R-DEHM	0.65	0.53	0.51	0.78	0.59	0.67	0.68
R-EMEP	0.67	0.52	0.47	0.80	0.60	0.69	0.54
R-MATCH	0.60	0.43	0.40	0.78	0.70	0.64	0.54
R-SILAM	0.62	0.44	0.46	0.71	0.48	0.66	0.54
RMSE-DEHM	1.29	1.52	1.87	0.16	0.23	0.17	323
RMSE-EMEP	2.25	1.52	2.14	0.13	0.19	0.15	516
RMSE-MATCH	4.06	1.93	2.63	0.23	0.12	0.16	516
RMSE-SILAM	1.90	3.41	2.67	0.22	0.21	0.16	516
Number stations	84	88	87	84	88	87	88

Notes: for any one site, deposition is the product of C_p × Precip, but here we present the averages across sites of each value.

ACPD
14, 6663–6720, 2014

Table 5. Base-case depositions of Nr (kg(N) ha^{-1}) components for the four CTMs, along with the 3CTM-ensemble mean and spread. Values are average depositions over the inner domain (see Fig. 1).

	DEHM	EMEP	MATCH	SILAM	3CTM-Ensemble mean	3CTM-Ensemble spread (%)
TDEP-Nr	9.0	6.7	7.2	7.1	7.0	8
TDEP-NO_y	4.0	3.1	3.5	4.2	3.6	31
TDEP-NH_x	5.0	3.6	3.7	2.9	3.4	22
WDEP-Nr	4.2	4.3	4.7	4.7	4.6	8
WDEP-NO_y	1.9	2.0	2.3	2.8	2.4	32
WDEP-NH_x	2.4	2.3	2.4	1.9	2.2	26
DDEP-Nr	4.7	2.3	2.5	2.4	2.4	9
DDEP-NO_y	2.1	1.0	1.3	1.4	1.2	27
DDEP-NH_x	2.6	1.3	1.3	1.1	1.2	19

Notes: the 3CTM ensemble consists of the the three European-scale CTMs driven by RCA3. Spread is defined as (max – min)/mean of these 3 models.

ACPD
14, 6663–6720, 2014

Table 6. Excess Nr-deposition over 10 kg(N) ha^{-1} yr^{-1} for the four CTMs in the EU28^{+} region.

Model	E05-M00-BC1		E05-M50-BC2		E05-M50-BC3		E50-M50-BC3		E50X20-M50-BC3		E50X30-M50-BC3	
	f_{10}	E_{10}	f_{10}	E_{10}	f_{10}	E_{10}	f_{10}	E_{10}	f_{10}	E_{10}	f_{10}	E_{10}
DEHM	56	3.58	56	3.75	55	3.74	38	2.09	45	3.18	–	–
EMEP	37	1.44	38	1.53	37	1.50	19	0.55	28	1.01	32	1.29
MATCH	43	2.41	43	2.44	44	2.46	28	1.04	–	–	–	–
SILAM	40	1.82	39	1.76	39	1.73	18	0.48	–	–	–	–

Notes: f_{10} gives the fraction (%) of EU28^{+} region with Nr-depositions in excess of 10 kg(N) ha^{-1}; E_{10} gives the mean value of excess deposition (kg(N) ha^{-1} yr^{-1}) averaged across the EU28^{+} region.

ACPD
14, 6663–6720, 2014

Table 7. Statistics of detailed critical load exceedances in the EU28^{+} region, EMEP MSC-W model.

Scenario	area exceeded f_{CL} (%)	mean exceedance E_{CL} (kg (N) ha^{-1} yr^{-1})
E05-M00-BC1	64.1	3.81
E05-M50-BC2	64.4	3.83
E05-M50-BC3	64.1	3.78
E50-M50-BC3	49.8	1.89
E50X20-M50-BC3	54.9	2.57
E50X30-M50-BC3	56.9	2.94

ACPD
14, 6663–6720, 2014

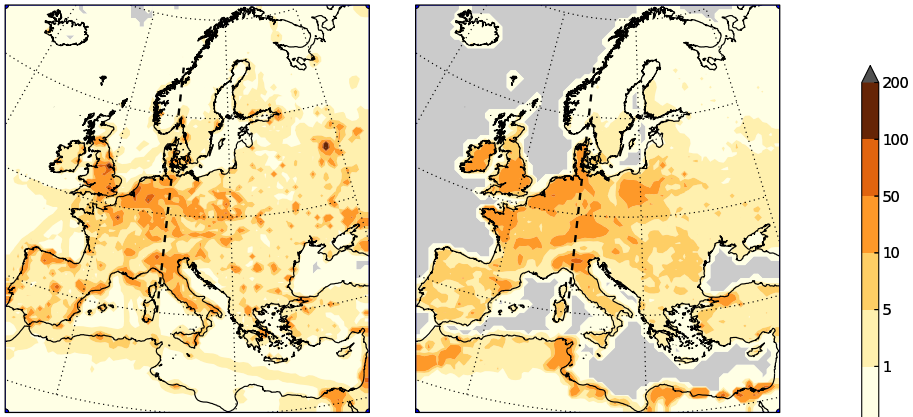

(a) NOx (b) NH_3

Fig. 1. Emissions of NO_x and NH_3 for the 2005 base-year, units kg(N) ha^{-1}. Also indicated is the transect-line through 10° E used in Figs. 8 and 9.

ACPD
14, 6663–6720, 2014

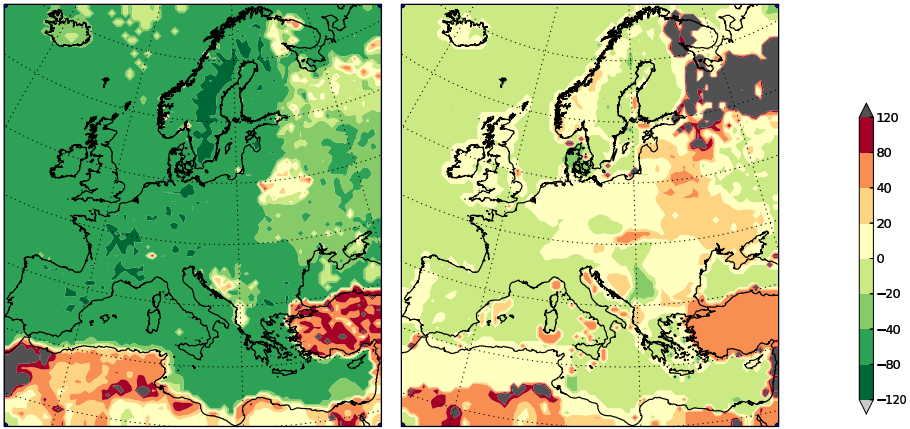

(a) NOx *(b)* NH_3

Fig. 2. Emissions changes (%), 2005 to 2050, of NO_x and NH_3.

ACPD
14, 6663–6720, 2014

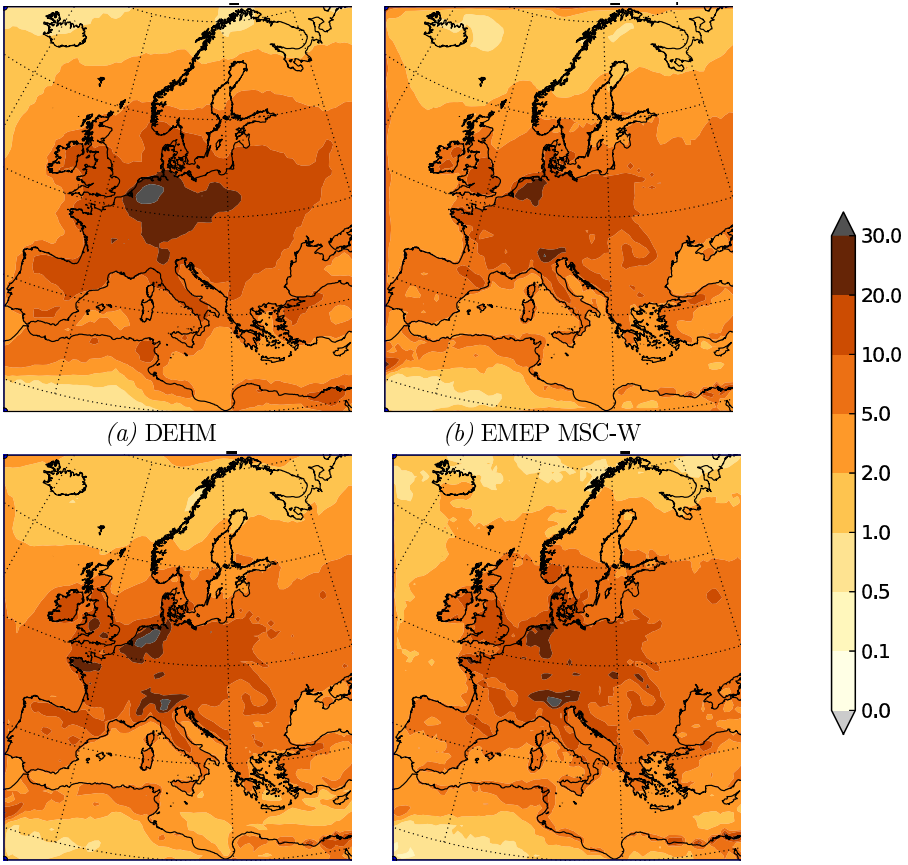

(a) DEHM (b) EMEP MSC-W

(c) MATCH (d) SILAM

Fig. 3. Calculated deposition of total Nr from the four CTMs. Results given as 20 yr means (1990–2009) for the base-case (E05-M00-BC1), units kg (N) ha^{-1}.

ACPD
14, 6663–6720, 2014

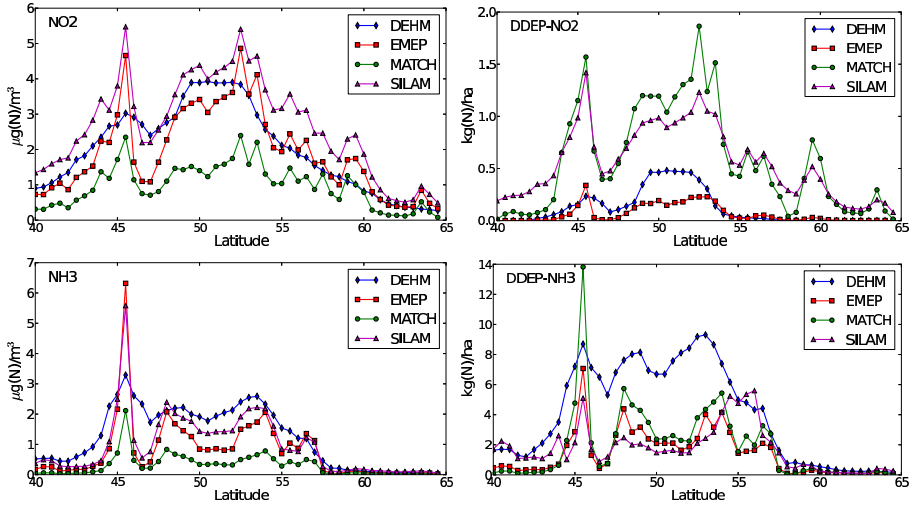

Fig. 4. Examples of model variability for two compounds. Calculated base-case concentrations (left column, $\mu g\,(N)\,m^{-3}$) and dry-depositions (right column, $kg\,(N)\,ha^{-1}$) along the 10° E transect (cf. Fig. 1), for NO_2 (top row) and NH_3 (bottom row).

ACPD
14, 6663–6720, 2014

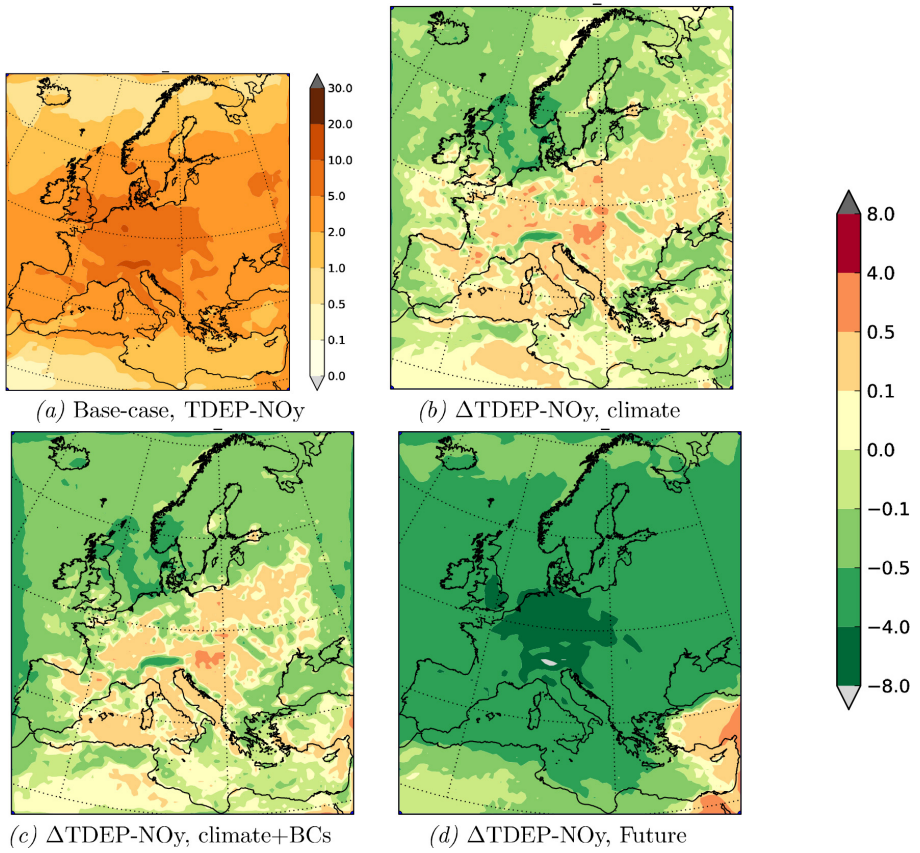

Fig. 5. Results from the 3-CTM ensemble (see text), for **(a)** base-case deposition of NO_y (TDEP-NO_y, innermost legend); and changes in TDEP-NO_y (rightmost legend) resulting from **(b)** 2050s climate (E05-M50-BC2), **(c)** 2050s climate and boundary conditions (E05-M50-BC3), **(d)** 2050s emissions, climate and boundary conditions (E50-M50-BC3). Units kg (N) ha^{-1}.

ACPD
14, 6663–6720, 2014

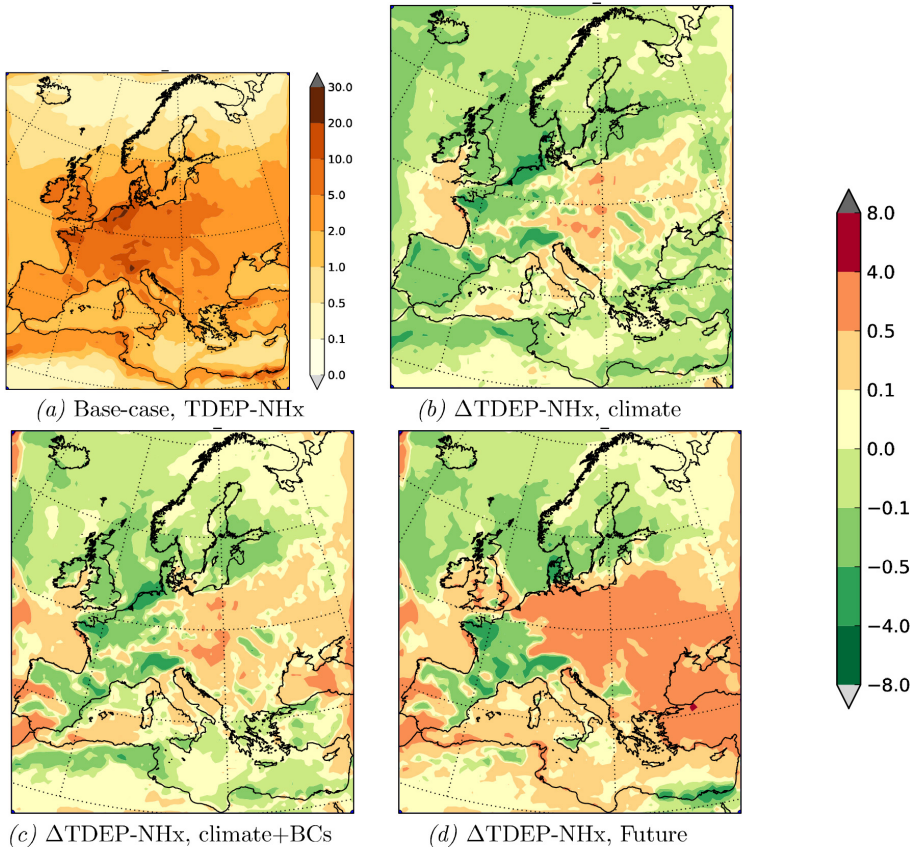

Fig. 6. As Fig. 5, but for reduced nitrogen, NH_x.

ACPD
14, 6663–6720, 2014

Impacts of climate and emission changes on nitrogen deposition

D. Simpson et al.

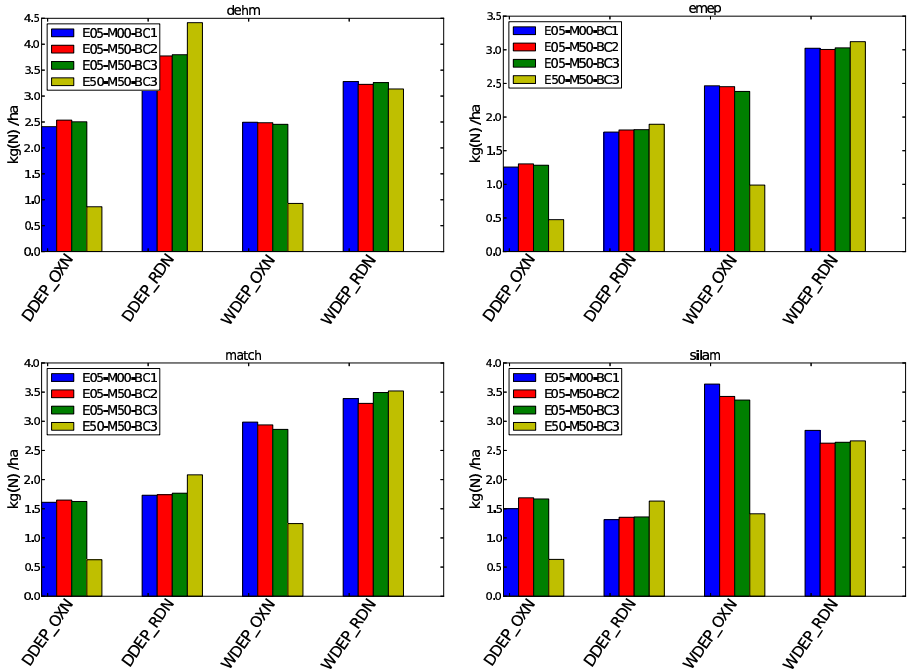

Fig. 7. Calculated deposition components of Nr from four CTMs and four scenarios. Blocks of bars distinguish wet and dry deposition (WDEP, DDEP) and NO_y and NH_x components.

ACPD
14, 6663–6720, 2014

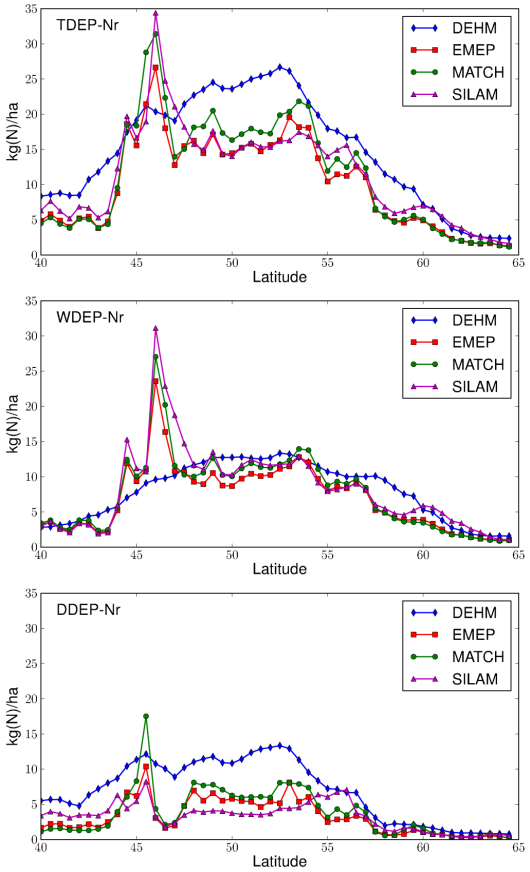

Fig. 8. Calculated base-case deposition along the 10° East transect (cf. Fig. 1), for total Nr deposition (top), wet-deposition (middle), dry deposition (bottom).

ACPD
14, 6663–6720, 2014

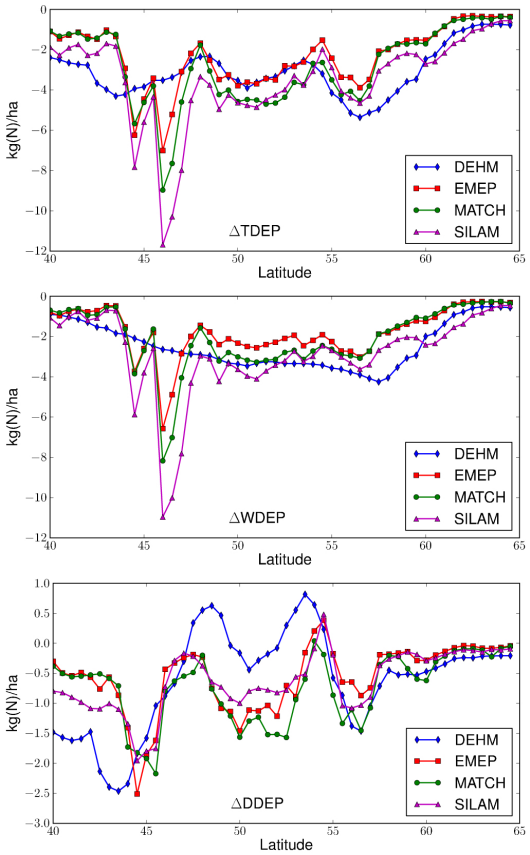

Fig. 9. Calculated changes in total, wet and dry deposition of Nr, future case (E50-M5-BC3) minus base-case (E05-M00-BC1). Same transect as Fig. 8.

ACPD
14, 6663–6720, 2014

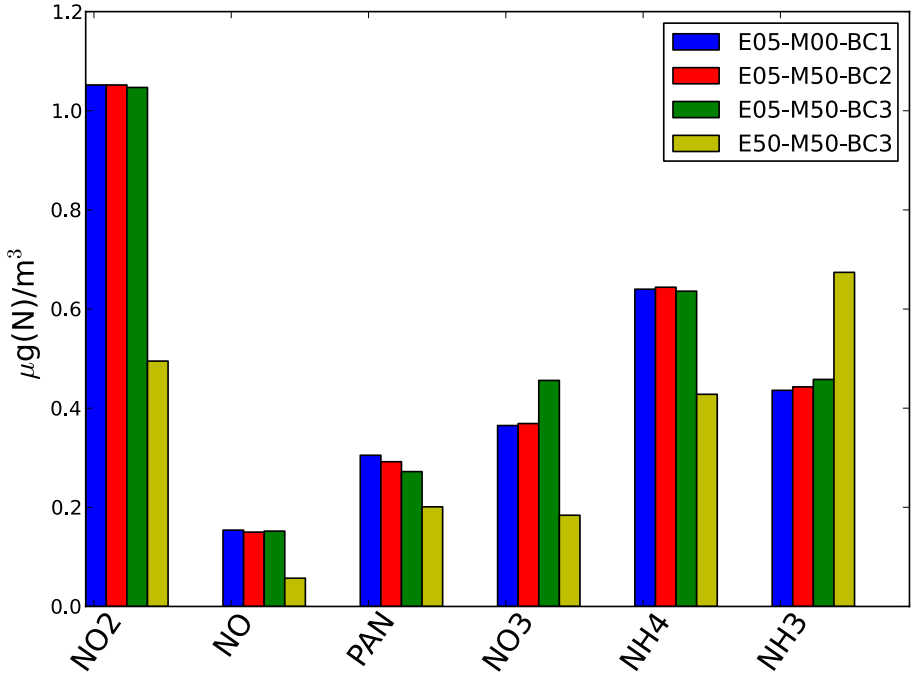

Fig. 10. Calculated concentrations of major Nr species from the EMEP MSC-W model for four scenarios.

ACPD
14, 6663–6720, 2014

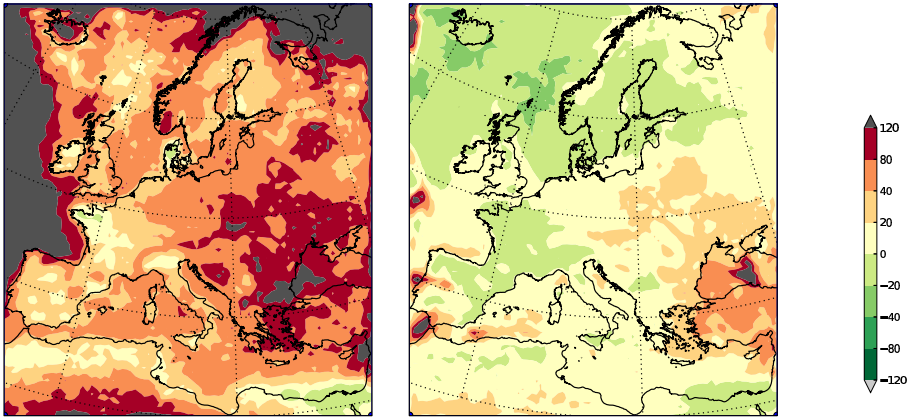

(a) NH_3 (b) NHx

Fig. 11. Changes in total deposition (%), from 2005 to 2050, for NH_3 and NH_x. Results from the 3CTM-ensemble. The colour-scale is identical to that used for emission changes in Fig. 2.

ACPD
14, 6663–6720, 2014

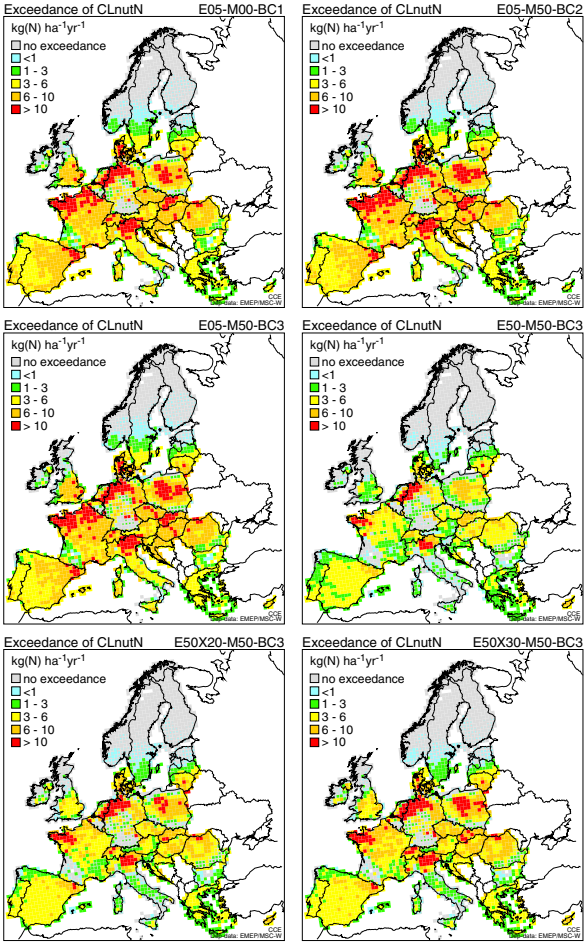

Fig. 12. Exceedances of the critical loads for nutrient nitrogen ($CL_{nut}(N)$) in the EU28^{+} region, EMEP MSC-W model, for the six scenarios.

ACPD
14, 6663–6720, 2014

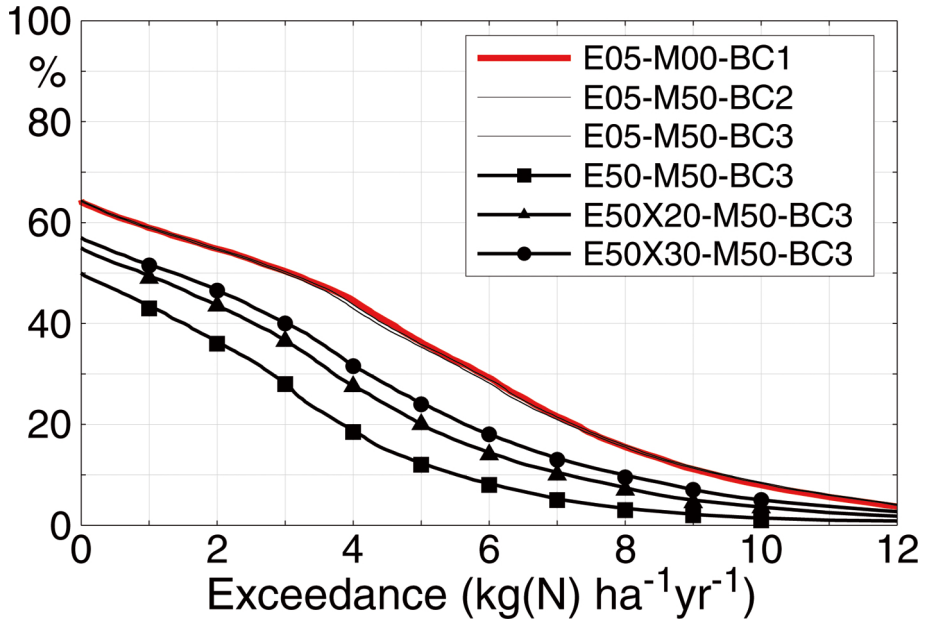

Fig. 13. Inverse cumulative distribution functions (cdfs) of exceedances (AAE) of $CL_{nut}(N)$ in $EU28^{+}$ for the 6 scenarios using the EMEP MSC-W model. Note that scenarios 2 and 3 (black thin lines) hardly differ from the base scenario.

ACPD
14, 6663–6720, 2014